



THE RADIATIVE CORRECTIONS TO THE ELECTROWEAK
PARAMETERS IN THE DOMINANT FERMION-LOOP APPROXIMATION

G. Gounaris^{*)}

Dept. of Physics, University of Bielefeld,
D-4800 Bielefeld 1, F.R. Germany

and

D. Schildknecht⁺⁾

CERN - Geneva

ABSTRACT

A simple treatment of the dominant radiative corrections to the W^+ and Z^0 mass formulae due to fermion-loop corrections to the propagator is given, including the possibility of a very massive top quark, $m_t > M_W$. A thorough comparison with the results of the complete $(SU(2)_L \times U(1)_Y)$ one-loop calculations is presented. Using α , G_μ and M_Z as input, we find excellent agreement with the complete one-loop calculations (with $m_{\text{HIGGS}} \cong 100$ GeV) for all values of m_t within an expected error of $\Delta M_W \cong (\alpha/2\pi)M_W \cong 100$ MeV in M_W and $\Delta s_W^2 \cong 0.002$ in the weak angle, s_W^2 . Technically we differ from previous work in diagonalizing the γZ propagator for arbitrary values of q^2 , thus allowing for extensive use of the notion of "running" coupling constants and masses. We also give a simple and closed formula for the radiative corrections to be applied to s_W^2 (accurate within an expected error of $\Delta s_W^2 \cong 0.002$), when extracting s_W^2 from neutrino scattering experiments. As a strategy for future precision tests of the electroweak theory, we suggest attempting to isolate and to test directly the "new physics" of boson loops and other new phenomena by comparing with and looking for deviations (larger than $\Delta M_W \cong (\alpha/2\pi)M_W$) from the predictions of the dominant fermion-loop calculation.

*) Partially supported by Deutsche Forschungsgemeinschaft.

Permanent address: Dept. of Theoretical Physics, University of Thessaloniki, Thessaloniki, Greece.

+) Permanent address: Dept. of Physics, University of Bielefeld, D-4800 Bielefeld 1, F.R. Germany.

1. Introduction

Quantum corrections to the masses and couplings of the weak vector bosons are dominated by fermion loop contributions to the propagators of the W^\pm and the γZ system. This is a well-known fact. It becomes apparent within the complete one-loop calculations of the radiative corrections¹⁻³⁾ in the $SU(2)_L \times U(1)_Y$ spontaneously broken electroweak gauge theory⁴⁾ as well as in the approximate treatment which takes into account the leading (logarithmic) corrections^{5-7,*)} only.

In the present work we concentrate on the dominant lepton and quark-loop corrections to the W^\pm and γZ propagators. Our basic motivation may be summarized as follows: fermion-loop corrections to the vector boson masses and couplings can be reliably calculated. They only depend on the masses and the couplings of the leptons and quarks to the vector bosons. Both masses and couplings are empirically known apart from the mass (and the couplings) of the top quark, m_t , which has to be treated as a free parameter allowing for values^{9,10)} of m_t even larger than the W^\pm mass, $m_t > M_W$. Boson-loop corrections, on the other hand, in general depend on the empirically completely unknown self-couplings of the vector bosons and the unknown value of the mass of the Higgs scalar, m_H . While being suppressed and small compared with the fermion-loop corrections as long as m_H is small, i.e., for $m_H \approx M_W$, boson-loop corrections may become very large for $m_H \gg 1$ TeV, so large even that a perturbative treatment starts to become unreliable. A value of $m_H \gg 1$ TeV corresponds to a strongly interacting sector^{11,12)} within the $SU(2)_L \times U(1)_Y$ theory which a priori cannot be excluded at present. Vector-boson-loop corrections are also most likely to differ from the conventionally calculated ones if, e.g., vector bosons are of composite nature implying the existence of a spectrum of isoscalar and excited bosons which modify the loop corrections. One may conclude that boson-loop corrections at present are more model-dependent than the largely model-independent fermion-loop corrections. There is thus every reason for performing a transparent calculation of the dominant fermion-loop corrections by themselves. A thorough comparison of the magnitude of the corrections thus obtained with the results of the complete one-loop calculations¹³⁻¹⁷⁾ is essential for precisely establishing the accuracy which will most likely be needed in order to isolate and directly test

* For reviews on radiative corrections to the electroweak parameters see, e.g., ref. 8.

contributions due to the bosonic sector of the electroweak theory, which in fact contains the "new" (empirically unknown) physics in contrast to the "old" physics of the interactions of the vector bosons with the leptons and quarks.

The fermion-loop corrections to the propagators are enhanced by large logarithms, typically of the order of $(\alpha/\pi) \cdot \ln(M_W/m_\mu) \cong (\alpha/\pi) \cdot 6.6$. Bosonic propagator and vertex corrections in the $SU(2)_L \times U(1)_Y$ theory are expected to be of the order of α/π , as long as the Higgs mass is small, $m_H \cong M_W$. As long as boson-loop corrections are disregarded, it is thus sufficient for a consistent calculation to treat the light fermions in the leading log approximation, taking into account, however, the possibility of a very heavy top quark, $m_t \gg M_W$, which is known to contribute an important term⁹⁾ proportional to m_t^2 as well as a term proportional to $\ln(m_t/M_W)$.

Our treatment of the fermion-loop corrections to the W^\pm and γZ propagators is a novel one, insofar as the leading contributions are calculated by using propagator methods rather than the familiar renormalization group methods. Effects of a large mass of the top quark, $m_t > M_W$, can thus be easily incorporated. By diagonalizing the γZ propagator matrix for arbitrary values of q^2 , the procedure of absorbing radiative propagator corrections in q^2 -dependent ("running") coupling constants and masses is generalized from the case of the propagator of a single particle to the present case of a two-by-two propagator matrix. As a result we obtain a simple and intuitively transparent treatment of the fermion loop corrections to the propagators in terms of q^2 -dependent coupling constants, W^\pm and Z masses and q^2 -dependent widths. Among other things, it is clarified why the Fermi coupling, G_μ , "does not run", i.e., is a "good" high energy parameter, how the tree-level relations for, e.g., $\sin^2\theta_W$ are affected by the presence of a very massive top quark and how the vector boson widths, $\Gamma_{W,Z}$, depend on q^2 , thus affecting the Z-line shape, etc.

As regards neutrino scattering, simple and closed formulae will be given within our approximation to be applied easily when extracting $\sin^2\theta_W$ from the experimental data.

The paper is subdivided as follows: Section 2 contains the study of the fermion-loop corrections to the W^\pm and γZ propagators. Details on the renormalization and the novel treatment of the diagonalization of the γZ propagator matrix are deferred to Appendices A and B. In Section 3 we will discuss the numerical predictions for M_W and $\sin^2\theta_W$ for a series of reasonable choices of M_Z and m_t , and compare these predictions with the corresponding results of a full one-loop calculation available in the literature^{14,15)} (compare Table 1 and Fig. 2). In

Section 4 we will give our closed formulae for the radiative corrections to be applied when extracting $\sin^2\theta_W$ from neutrino-hadron and neutrino-electron scattering experiments. A comparison of our results with the ones of a full one-loop calculation is also given for this case (compare Table 2). Section 5 contains our summarizing conclusions.

2. The Vector-Boson Propagators

The radiative corrections to the W^\pm and γZ propagators for values of q^2 in the range of

$$0 \lesssim |q^2| \lesssim M_W^2 \cong M_Z^2 \quad , \quad (2.1)$$

where M_W and M_Z denote the measured W^\pm and Z masses, are mainly due to fermion loops. The relevant Feynman diagrams are shown in Fig. 1. Compared with the contributions of the lepton and quark loops, which are enhanced by logarithms of the ratios of vector-boson to lepton and quark masses, the vector-boson-loop contributions are small for the values of $|q^2|$ indicated in (2.1). This suppression of the boson-loop corrections is true, provided the effective cut-off in the relevant Feynman diagrams is of the order of M_W . This latter condition is readily satisfied in the $SU(2)_L \times U(1)_Y$ theory for a mass of the Higgs scalar of the order of M_W leading to boson-loop corrections of the order of α/π or at most of the order of α_W/π . The same situation occurs in effective electroweak theories based on γW^3 mixing¹⁸⁾ and W -dominance^{19,20)}, provided the effective cut-off of the theory is sufficiently small. We thus expect that also in this approach the diagrams in Fig. 1 give all the relevant corrections to the W^\pm and γZ propagators within the q^2 range indicated in (2.1).

In calculating the lepton and quark loops of Fig. 1, all fermions lighter than $M \cong M_W \cong M_Z$ are treated as massless, retaining their leading contribution of the form $\ln(|q^2|/M^2)$ only. Threshold corrections due to the finite masses of these particles are introduced only at the very end⁶⁾. The unknown and possibly very large mass of the top quark, m_t , is treated as a free parameter. For $m_t \gg M$ the dominant top quark contribution arises from the quadratically divergent part of the diagram in Fig. 1 and is proportional⁹⁾ to m_t^2 . In addition there is a term proportional to $\ln(m_t/M)$ from the logarithmically divergent part of the diagram.

After renormalization (compare Appendix A for a brief summary), the transverse part of the W^\pm propagator multiplied by the strength of the coupling to the external fermions in Fig. 1 is given by^{*}

$$\alpha_W(M_W^2) \Delta_{\mu\nu}^W(q^2) = \frac{-i \alpha_W(M_W^2)}{q^2(1 + \Pi_W(q^2)) - M_W^2} T_{\mu\nu} \quad , \quad (2.2)$$

* We only consider the transverse part of the W^\pm -propagator. The longitudinal part is ignored, as in connection with our present discussion only interactions with light external fermions are of importance.

where

$$T_{\mu\nu} = g_{\mu\nu} - \frac{q_\mu q_\nu}{q^2} \quad , \quad (2.3)$$

and the vacuum polarization function, $\Pi_W(q^2)$, fulfills

$$\text{Re } \Pi_W(M_W^2) = 0 \quad . \quad (2.4)$$

Condition (2.4) is a consequence of renormalizing at the scale M_W . It guarantees that the zero of the real part of the inverse of the propagator coincides with the physical W^\pm mass, M_W , and thus the residue of the pole, $\alpha_W(M_W^2) \equiv g_W^2(M_W^2)/4\pi$ is identical to the W^\pm fermion coupling at the scale M_W . Explicitly we have

$$\Pi_W(q^2) = -\alpha_W(M_W^2) b_i \cdot \begin{cases} A(q^2) - \frac{1}{3} \cdot i & \text{for } q^2 > 0 \\ A(q^2) & \text{for } q^2 < 0 \end{cases} \quad , \quad (2.5)$$

with

$$A(q^2) = \frac{1}{3\pi} \ln\left(\frac{|q^2|}{M^2}\right) \quad (2.6)$$

and

$$b_i = \frac{1}{2} \sum_i \left(\frac{\tau_3^i}{2} \right) = \frac{1}{4} n = \begin{cases} 3 & \text{for } m_t < M_W \\ 9 & \text{for } m_t > M_W \end{cases} \quad , \quad (2.7)$$

where

$$\tau_3^i = \begin{cases} +1 & \text{for } \nu, u, \text{ etc.} \\ -1 & \text{for } e, d, \text{ etc.} \end{cases} \quad . \quad (2.7a)$$

The sum in (2.7) runs over all fermions which belong to doublets with both members of the doublet lighter than M_W , i.e., n , which is identical to the number of contributing doublets, is equal to $n = 12$ for $m_t < M_W$, while $n = 9$ for $m_t > M_W$.

Using the expression (2.5) for $\Pi_W(q^2)$ and multiplying the numerator and the denominator in (2.2) by $(1 + \text{Re } \Pi_W(q^2))^{-1}$, the W propagator may be rewritten in the form

$$\alpha_W(M_W^2) \Delta_{\mu\nu}^W(q^2) = \frac{i \alpha_W(q^2)}{q^2 - M_W^2(q^2) + i \Gamma_W(q^2) M_W(q^2)} \quad , \quad (2.8)$$

where by definition

$$\alpha_W(q^2) = \frac{\alpha_W(M_W^2)}{1 - \alpha_W(M_W^2) b_i A(q^2)} \quad , \quad (2.9)$$

as well as

$$M_W^2(q^2) = \frac{M_W^2}{1 - \alpha_W(M_W^2) b_1' A(q^2)} = M_W^2 \frac{\alpha_W(q^2)}{\alpha_W(M^2)}, \quad (2.10)$$

and, finally,

$$\Gamma_W(q^2) = \begin{cases} \frac{q^2}{M_W} \frac{\alpha_W(M_W^2)}{3} b_1' & \text{for } q^2 > 0 \\ 0 & \text{for } q^2 < 0 \end{cases}. \quad (2.11)$$

The physical interpretation of (2.8) is simple. Fermion-loop corrections to the propagator are taken into account by introducing a q^2 -dependent coupling, mass and width of the vector boson. We note that the q^2 dependence ("running") of $\alpha_W(q^2)$ and $M_W(q^2)$ is a logarithmic one, while $\Gamma_W(q^2)$ varies linearly * with q^2 . This linear dependence on q^2 is due to the q^2 factor multiplying $\Pi_W(q^2)$ in (2.2). The width becomes quickly negligible for $q^2 < M_W^2$.

An important physical consequence can now immediately be obtained from (2.8). Employing the propagator (2.8) to describe muon decay, (2.8) has to be evaluated in the limit of $q^2 \approx 0$. Consequently, the $q^2 \rightarrow 0$ limit of the propagator (2.8) may be directly identified with the experimentally measured** Fermi coupling, G_μ . Noting in addition that according to (2.9) and (2.10) the ratio of $\alpha_W(q^2) / M_W^2(q^2)$ is independent of q^2 , we find that

$$\frac{\sqrt{2}}{\pi} G_\mu = \frac{\alpha_W(0)}{M_W^2(0)} = \frac{\alpha_W(M_W^2)}{M_W^2}. \quad (2.12)$$

The tree-level relationship between G_μ , the W coupling to fermions, $\alpha_W(M_W^2)$, measured at the physical W mass and the W mass itself remains intact, even when fermion-loop corrections to the propagator are taken into account; the Fermi coupling, G_μ , determined by muon decay at low energies ($|q^2| \ll M_W^2$) measures directly the ratio of the on-mass-shell coupling of the W to fermions, $g_W(M_W^2)$, and the physical W mass. It is exactly this important point which allows one to predict the high-energy parameters $g_W(M_W^2)$ and M_W from the low-energy parameter G_μ . The argument which led to (2.12) substantiates the usual jargon that G_μ is a "good high energy parameter" since "it does not run".

Next, we focus on the γZ propagator which is calculated according to the dia-

* This conclusion is based on the definition of the width given by (2.8) and is at variance with ref.21 .

** When extracting G_μ from muon decay an (ultra-violet finite) QED correction is taken into account.

grams of Fig. 1b. As the fermion loops induce γZ mixing terms, the propagator becomes a two-by-two propagator matrix which in general has off-diagonal elements. A repetition of the above procedure of absorbing loop corrections in q^2 -dependent coupling constants and masses requires a diagonalization of this γZ propagator matrix for arbitrary q^2 . Once the propagator matrix is brought into diagonal form*, one may introduce q^2 -dependent photon and Z-boson couplings to the fermions and a q^2 -dependent Z-boson mass as well as a q^2 -dependent width in analogy to the case of the W treated above.

After renormalization at the scale $M \cong M_W \cong M_Z$ (compare Appendix A) the transverse part of the inverse propagator matrix of the γZ system takes the form (compare (A29))

$$-i(\Delta^{\gamma Z})_{\mu\nu}^{-1} = T_{\mu\nu} [q^2(1 + \Pi_{\gamma Z}(q^2)) - M_{\gamma Z}^2] \quad . \quad (2.13)$$

This propagator is to be used in conjunction with the current doublet (compare (A32))

$$j_\mu = \begin{pmatrix} e(M^2) j_\mu^{\text{em}} \\ g_Z(M^2) (j_\mu^{(3)} - \bar{s}_W^2(M^2) j_\mu^{\text{em}}) \end{pmatrix} \quad , \quad (2.14)$$

which defines the coupling constants at the scale M^2 .

In (2.13), the vacuum polarization matrix, $\Pi_{\gamma Z}(q^2)$, is given by (compare (A30) and (A31))

$$\Pi_{\gamma Z}(q^2) = -\frac{\alpha(M_Z^2)}{3\pi} \ln\left(-\frac{q^2}{M_Z^2}\right) \begin{pmatrix} b_Q \quad , \quad \frac{b_2 - \bar{s}_W^2 b_Q}{\bar{s}_W \bar{c}_W \sqrt{d}} \\ \frac{b_2 - \bar{s}_W^2 b_Q}{\bar{s}_W \bar{c}_W \sqrt{d}} \quad , \quad \frac{b_1 + \bar{s}_W^4 b_Q - 2\bar{s}_W^2 b_2}{\bar{s}_W^2 \bar{c}_W^2 d} \end{pmatrix} \quad , \quad (2.15)$$

where the constants b_1 , b_2 and b_Q are related to the weak isospin, $\tau_3^{(i)}$, and the charges, Q_i , of the contributing leptons and quarks via

$$b_1 = \frac{1}{2} \sum_i (\frac{\tau_3^{(i)}}{2})^2 \quad ,$$

* In terms of the fields defining the propagator, its diagonalization corresponds to a transition from the original renormalized photon and Z fields (i.e., existence of γZ mixing terms for $q^2 \neq M_Z^2$) to new "running" fields for the photon and the Z-boson.

$$b_2 = \sum_i Q_i \frac{\tau_3^{(i)}}{4} ,$$

$$b_Q = \sum_i Q_i^2 . \quad (2.16)$$

The sums run over all leptons and quarks with masses m_i smaller than M_W which are treated as massless at this stage. We thus have $(b_1, b_2, b_Q) = (24/8, 24/8, 24/3)$ for $m_t < M_W$, while $(b_1, b_2, b_Q) = (21/8, 20/8, 20/3)$ for $m_t > M_W$. The correction factor d in (2.16) is given by

$$d = 1 + \frac{\alpha_W(M_Z^2)}{24\pi \bar{c}_W^2} \ln \frac{m_t^2}{M_Z^2} . \quad (2.17)$$

For M_Z in (2.13) we have

$$M_{YZ}^2 = \begin{pmatrix} 0 & 0 \\ 0 & M_Z^2 \end{pmatrix} \quad (2.18)$$

with (compare (A37))

$$M_Z^2 = \begin{cases} \frac{M_W^2}{\bar{c}_W^2} & \text{for } m_t < M_W \\ \frac{M_W^2}{\bar{c}_W^2} \left(1 + \frac{3\alpha_W(M^2)}{16\pi} \frac{m_t^2}{M_W^2} + \frac{\alpha_W(M^2)}{24\pi \bar{c}_W^2} (1 + 2\bar{c}_W^2) \ln \frac{m_t^2}{M_W^2} \right)^{-1} & \text{for } m_t > M_W \end{cases} . \quad (2.19)$$

Here as well as in the ensuing considerations we used the asymptotic formulae derived for $m_t \gg M_W$ in the whole range of $m_t > M_W$. Due to

$$\text{Re } \Pi_{YZ}(M_Z^2) = 0 , \quad (2.20)$$

the zero of the real part of the inverse of the Z propagator correctly coincides with the empirical mass, M_Z , of the Z boson.

In (2.14) we have introduced the electromagnetic coupling $e(M^2)$ at the scale $M^2 \cong M_W^2 \cong M_Z^2$ as well as the Z coupling to leptons and quarks, $g_Z(M^2)$, and the weak angle, $\bar{s}_W^2 \equiv \bar{s}_W^2(M^2)$ at the scale M^2 . The electromagnetic fine-structure constant measured at the scale M^2 is thus given by

$$\alpha(M^2) = \frac{e^2(M^2)}{4\pi} , \quad (2.21)$$

and according to (A34) we have

$$\bar{s}_W^2 \equiv \bar{s}_W^2(M^2) = \begin{cases} \frac{\alpha(M^2)}{\alpha_W(M^2)} & \text{for } m_t < M_W \\ \frac{\alpha(M^2)}{\alpha_W(M^2)} \left(1 + \frac{\alpha_W(M^2)}{12\pi} \ln \frac{m_t^2}{M_W^2} \right) & \text{for } m_t > M_W \end{cases} , \quad (2.22)$$

while the Z coupling to leptons and quarks is given by

$$\alpha_Z(M^2) = \begin{cases} \frac{\alpha(M^2)}{\bar{s}_W^2 \bar{c}_W^2} = \frac{\alpha_W(M^2)}{\bar{c}_W^2} & \text{for } m_t < M_W \\ \frac{\alpha(M^2)}{\bar{s}_W^2 \bar{c}_W^2 \left(1 + \frac{\alpha_W(M^2)}{24\pi \bar{c}_W^2} \ln \frac{m_t^2}{M_W^2}\right)} = \frac{\alpha_W(M^2)}{\bar{c}_W^2 \left(1 + \frac{\alpha_W(M^2)}{24\pi \bar{c}_W^2} (1 + 2\bar{c}_W^2) \ln \frac{m_t^2}{M_W^2}\right)} & \text{for } m_t > M_W \end{cases} \quad (2.23)$$

According to (2.19), (2.22) and (2.23), as long as $m_t < M_W$, in our approximation the radiative corrections induced by lepton and quark loops do not affect the tree-level relations for M_Z^2 , \bar{s}_W^2 and α_Z defined at the scale M . For $m_t > M_W$, the tree-level relation for M_Z^2 receives a correction which depends quadratically and logarithmically on m_t , while \bar{s}_W^2 and $\alpha_Z(M^2)$ are corrected by logarithmic terms only.

The deviation from the tree-level relation between M_W and M_Z in (2.19) for $m_t > M_W$ may be expressed in terms of the parameter $\bar{\rho}$ defined by

$$\bar{\rho} \equiv \frac{M_W^2}{\bar{c}_W^2 M_Z^2} = \begin{cases} 1 & \text{for } m_t < M_W \\ 1 + \frac{3\alpha_W(M^2) m_t^2}{16\pi M_W^2} + (1 + 2\bar{c}_W^2) \frac{\alpha_W(M^2)}{24\pi \bar{c}_W^2} \ln \frac{m_t^2}{M_W^2} & \text{for } m_t > M_W \end{cases} \quad (2.24)$$

A large mass of the top quark thus implies $\bar{\rho} > 1$. Using

$$\delta\bar{\rho} \equiv \bar{\rho} - 1 \quad (2.25)$$

one may relate \bar{s}_W^2 introduced by (2.14) (as the coefficient of the contribution of j^{em} to the neutral current) to the frequently used weak angle s_W^2 defined by the ratio of the W^\pm and Z masses according to³⁾

$$s_W^2 \equiv 1 - \frac{M_W^2}{M_Z^2} \quad (2.26)$$

In lowest order in $\delta\bar{\rho}$ one immediately obtains

$$\begin{aligned} s_W^2 &= \bar{s}_W^2 - \bar{c}_W^2 \delta\bar{\rho} \quad , \\ \bar{c}_W^2 &= \bar{c}_W^2 \bar{\rho} \quad , \end{aligned} \quad (2.27)$$

and thus

$$\begin{aligned} \bar{s}_W^2 &= s_W^2 + \bar{c}_W^2 \delta\bar{\rho} \quad , \\ \bar{c}_W^2 &= \bar{c}_W^2 (1 - \delta\bar{\rho}) \quad . \end{aligned} \quad (2.28)$$

For $m_t < M_W$ we have $\bar{\rho} = 1$, s_W^2 in this case coincides with \bar{s}_W^2 , and all tree-level

relations remain intact upon introducing fermion-loop corrections. For $m_t > M_W$, all tree-level relations between (on-shell) coupling constants and masses receive corrections. Using (2.27) we may express $\delta\bar{\rho}$ in (2.24) within our approximation in terms of c_W^2 , rather than \bar{c}_W^2 by

$$\bar{\rho} = 1 + \frac{3\alpha_W(M^2) m_t^2}{16\pi M_W^2} + (1 + 2c_W^2) \frac{\alpha_W(M^2)}{24\pi c_W^2} \ln \frac{m_t^2}{M_W^2}, \quad (2.29)$$

a formula which will be used in the numerical evaluation of Section 3.

For $q^2 \neq M_Z^2$ not only the imaginary part but also the real part of the inverse propagator in (2.13) has non-vanishing off-diagonal elements. Using the method of Appendix B the real part of the propagator matrix is now cast into diagonal form for any value of q^2 . The effect of the fermion-loop corrections is thus reduced to the introduction of q^2 -dependent coupling constants and masses to be used in conjunction with a diagonal γZ propagator.

The diagonalization is achieved with the help of the transformation matrix D given by (B12) with appropriately defined (q^2 -dependent) parameters c_1 , c_2 and λ . These parameters are identified by comparing the real part of $(1 + \Pi_{\gamma Z}(q^2))$ in (2.13) with the matrix K in (B2). The matrix element of the γZ propagator becomes

$$j_\mu^+(\Delta^{\gamma Z})^{\mu\nu} j_\nu = j_\mu^+ D^t \begin{pmatrix} \frac{1}{q^2} & 0 \\ 0 & \frac{1}{q^2 - M_Z^2(q^2) - i M_Z(Q^2) \Gamma_Z(q^2)} \end{pmatrix} D j^\mu, \quad (2.30)$$

where the transformed current is given by

$$D j_\mu = \begin{pmatrix} e(q^2) j_\mu^{em} \\ g_Z(q^2) [j_\mu^{(3)} - \bar{s}_W^2(q^2) j_\mu^{em}] \end{pmatrix}. \quad (2.31)$$

Using (B14) one explicitly finds the expressions for the q^2 -dependent coupling constants in (2.31). First of all,

$$\alpha(q^2) \equiv \frac{e^2(q^2)}{4\pi} = \frac{\alpha(M^2)}{1 - \alpha(M^2) b_0 A(q^2)}, \quad (2.32)$$

where $A(q^2)$ is given by (2.6). It is worth noting that formula (2.32) for the

"running" of $\alpha(q^2)$ coincides with the well-known result obtained if one considers loop corrections to the photon propagator by itself. The q^2 dependence of $\alpha(q^2)$ is thus unaffected by the presence of the γZ mixing terms. Again using (B14) one finds

$$\begin{aligned}\bar{s}_W^2(q^2) &= \frac{\alpha(q^2)}{\alpha(M^2)} (\bar{s}_W^2(M^2) - \alpha(M^2) b_2 A(q^2)) = \\ &= \frac{\alpha(q^2)}{\alpha_W(q^2)} [1 + \alpha_W(q^2) ((b_1' - b_2) A(q^2) + \frac{1}{12\pi} \ln \frac{m_t^2}{M^2})] \end{aligned} \quad (2.33)$$

and

$$\begin{aligned}\alpha_Z(q^2) &\equiv \frac{g_Z^2(q^2)}{4\pi} = \\ &= \left(\frac{\bar{s}_W^2(q^2) \bar{c}_W^2(q^2)}{\alpha(q^2)} + (b_2 - b_1) A(q^2) + \frac{\alpha_W(M^2) \bar{s}_W^2(M^2)}{\alpha(M^2)} \frac{1}{24\pi} \ln \frac{m_t^2}{M^2} \right)^{-1}. \end{aligned} \quad (2.34)$$

These formulae hold for $m_t > M_W$. For $m_t < M_W$, the terms proportional to $\ln m_t^2$ have to be dropped. Moreover, for $m_t < M_W$ we have $b_1' = b_1 = b_2$ according to (2.7) and (2.16), and thus all the q^2 -dependent coupling constants, $\alpha(q^2)$, $\alpha_W(q^2)$, $\alpha_Z(q^2)$ and $\bar{s}_W^2(q^2)$ fulfil the same relations which are valid for the q^2 -independent quantities in the tree approximation. We also note that for $q^2 = M^2$ $A(M^2) = 0$, which implies that (2.33) and (2.34) correctly coincide with (2.22) and (2.23).

We return to (2.30) and also give the explicit expressions for $M_Z^2(q^2)$ and $\Gamma_Z(q^2)$. According to (B7) and (B14), the Z mass and the Z coupling are affected in the same manner when applying the transformation D which diagonalizes the real part of the γZ propagator. Consequently, we have

$$M_Z^2(q^2) = M_Z^2 \frac{\alpha_Z(q^2)}{\alpha_Z(M^2)}, \quad (2.35)$$

or, equivalently,

$$\frac{\alpha_Z(q^2)}{M_Z^2(q^2)} = \frac{\alpha_Z(M^2)}{M_Z^2}, \quad (2.36)$$

i.e., the ratio of $\alpha_Z(q^2)/M_Z^2(q^2)$ is a constant independent of q^2 , in complete analogy to the constancy of the ratio $\alpha_W(q^2)/M_W^2(q^2)$ implied by (2.9) and (2.10) (compare also (2.12)). Noting that the left-hand side of (2.36) evaluated for $q^2 \rightarrow 0$ is identical to the normalization of the neutral current neutrino interactions, one concludes that these reactions directly determine the ratio of the on-mass-shell coupling and the mass of the Z. An important consequence now follows

immediately by combining (2.36) with (A38) and (2.12) to yield

$$\rho \equiv \frac{\alpha_Z(q^2)/M_Z^2(q^2)}{\alpha_W(q^2)/M_W^2(q^2)} = \frac{\alpha_Z(q^2 \approx 0)/M_Z^2(q^2 \approx 0)}{\alpha_W(q^2 \approx 0)/M_W^2(q^2 \approx 0)} =$$

$$= \begin{cases} 1 & \text{for } m_t < M_W \\ 1 + \frac{3\alpha_W(M^2)}{16\pi} \frac{m_t^2}{M_W^2} & \text{for } m_t > M_W \end{cases} \quad (2.37)$$

and

$$\frac{\alpha_Z(q^2)}{M_Z^2(q^2)} = \rho G_\mu \frac{\sqrt{2}}{\pi} \quad , \quad (2.38)$$

i.e., a large mass of the top quark leads to a deviation of the ratio ρ of the neutral to charged current normalizations from the value of $\rho = 1$ valid at tree-level and for the case of $m_t < M_W$. This is a consequence of the fact that a large mass splitting between the t and b quarks, $m_t > M_W \gg m_b$ in this respect acts in the same manner as, e.g., the introduction of additional Higgs scalars with weak isospin $I \neq 1/2$ (compare (A4) and (A20)).

Finally from (2.15) one finds for $\Gamma_Z(q^2)$ in (2.30) in complete analogy to $\Gamma_W(q^2)$ in (2.11),

$$\Gamma_Z(q^2) = \begin{cases} \frac{q^2}{M_Z} \frac{\alpha_Z(M_Z^2)}{3} (b_1 + s_W^4 b_Q - 2s_W^2 b_2) & \text{for } q^2 > 0 \\ 0 & \text{for } q^2 < 0 \end{cases} \quad , \quad (2.39)$$

where (2.23) was used and only terms of order α are kept. The factor q^2 in (2.39) may influence the Z-boson line shape to be measured at LEP.

In view of the numerical evaluation of the radiative corrections in Section 3, we now introduce the threshold effects due to the non-vanishing lepton and quark masses in the formulae (2.32) and (2.33) for $\alpha(q^2)$ and $\bar{s}_W^2(q^2)$. We note that a fermion of mass m_i yields a contribution to $\Pi_{YZ}(q^2)$ in (2.15) which is proportional to $\ln(|q^2|/M^2)$ for $m_i^2 \ll q^2 \ll M^2$, and a contribution proportional to $\ln(m_i^2/M^2)$ for $|q^2| \ll m_i^2 \ll M^2$. Accordingly, the finite lepton and quark masses are taken into account in $\alpha(q^2)$ and $\bar{s}_W^2(q^2)$ by substituting²²⁾ (for $|q^2| < M^2$)

$$b_Q A(q^2) \rightarrow \frac{1}{3\pi} \sum_i Q_i^2 \left[\ln\left(\frac{|q^2|}{m_i^2}\right) \Theta(|q^2| - m_i^2) + \ln\left(\frac{m_i^2}{M^2}\right) \Theta(M^2 - m_i^2) \right] \quad ,$$

$$b_2 A(q^2) \rightarrow \frac{1}{12\pi} \sum_i Q_i \tau_3^{(i)} \left[\ln\left(\frac{|q^2|}{m_i^2}\right) \Theta(|q^2| - m_i^2) + \ln\left(\frac{m_i^2}{M^2}\right) \Theta(M^2 - m_i^2) \right] , \quad (2.40)$$

where the sum is to be extended over all leptons and quarks. Thus, the top quark does not contribute for $m_t > M \cong M_W > \sqrt{|q^2|}$. Likewise we write for the $\bar{\rho}$ and ρ parameters in (2.29) and (2.37)

$$\bar{\rho} = 1 + \frac{\sqrt{2} G_\mu}{4\pi^2} \left(\frac{3}{4} m_t^2 + \frac{M_W^2}{6c_W^2} (1 + 2c_W^2) \ln \frac{m_t^2}{M_W^2} \right) \Theta(m_t - M_W) , \quad (2.41)$$

and

$$\rho = 1 + \frac{3\sqrt{2}}{16\pi^2} G_\mu m_t^2 \Theta(m_t - M_W) , \quad (2.42)$$

where (2.12) has been used.

We end this Section with a brief remark on the renormalization group differential equations for the q^2 -dependent coupling constants $\alpha_W(q^2)$ and $\alpha(q^2)$. Even though we have entirely based our treatment on directly analysing the fermion-loop contributions to the propagators, renormalization group differential equations are (obviously) valid for the q^2 -dependent coupling constants. On the basis of (2.9) and (2.6) we conclude

$$q^2 \frac{\partial}{\partial q^2} \left(\frac{1}{\alpha_W(q^2)} \right) = - \frac{1}{3\pi} b_1 , \quad (2.43)$$

where b_1 is given by (2.7), and

$$q^2 \frac{\partial}{\partial q^2} \left(\frac{1}{\alpha(q^2)} \right) = - \frac{1}{3\pi} b_0 . \quad (2.44)$$

The equation (2.43) for $\alpha_W(q^2)$ is at variance with the corresponding equation given in Ref. 6. We also note that renormalization group arguments by themselves do not provide the q^2 factor in the expressions for $\Gamma_W(q^2)$ and $\Gamma_Z(q^2)$ given in (2.11) and (2.39). In fact, the renormalization group arguments of Refs. 6 and 21 provide a q^2 dependence for a definition of the W and Z widths which is unrelated to the imaginary part of the inverse propagator and thus has nothing to do with the Z line shape to be observed in e^+e^- experiments.

3. Numerical Predictions

As the Z mass, M_Z , will be precisely measured at LEP, it has become customary to use M_Z in conjunction with the Fermi constant, G_μ , and the electromagnetic fine structure constant, α , to predict the other electroweak parameters, in particular the W mass, M_W , and the ratio of M_W and M_Z which defines the conventionally used parameter

$$s_W^2 = 1 - M_W^2/M_Z^2 \quad . \quad (3.1)$$

The relevant formulae are easily obtained by collecting the different results of Section 2.

Using (2.12) and (2.22) which relate G_μ to the on-mass-shell coupling constant $\alpha_W(M^2) = g_W^2/4\pi$, and $\alpha_W(M^2)$ to $\alpha(M^2)$ and $\bar{s}_W^2(M^2)$, where $\bar{s}_W^2(M^2)$ is defined by (2.14), one obtains

$$\frac{\sqrt{2}}{\pi} G_\mu = \frac{\alpha(M^2)}{\bar{s}_W^2(M^2) M_W^2} \left(1 + \frac{\alpha_W(M^2)}{12\pi} \ln \frac{m_t^2}{M_W^2} \right) \quad (\text{for } m_t > M_W) \quad . \quad (3.2)$$

We now express \bar{s}_W^2 according to (2.28) in terms of s_W^2 and the deviation, $\delta\bar{\rho}$, of the $\bar{\rho}$ parameter (2.41) from $\bar{\rho} = 1$ and introduce the ratio $\alpha(0)/\alpha(M^2)$ given by (2.32). Relation (3.2) then becomes

$$M_W^2 = \left(\frac{\alpha(0)}{\sqrt{2}} \pi \right) \frac{1}{s_W^2(M^2) (1 - \Delta r)} \quad , \quad (3.3)$$

where the conventional notation $1 - \Delta r$ has been introduced for the factor by which the formula for M_W^2 differs from the tree-level relation. The correction $1 - \Delta r$ in our approximation of keeping the dominant fermion contributions only is given by

$$1 - \Delta r = \begin{cases} \frac{\alpha(0)}{\alpha(M^2)} & \text{for } m_t < M_W \\ \frac{\alpha(0)}{\alpha(M^2)} + \frac{c_W^2}{s_W^2} \frac{\sqrt{2} G_\mu}{4\pi^2} \left[\frac{3m_t^2}{4} + (3 - 4s_W^2) \frac{M_Z^2}{6} \ln \frac{m_t^2}{M_W^2} \right] & \text{for } m_t > M_W \end{cases} \quad , \quad (3.4)$$

where from (2.32) and (2.40) we obtain

$$\begin{aligned} \frac{\alpha(0)}{\alpha(M^2)} &= 1 + \alpha(0) b_Q A(q^2 \rightarrow 0) \\ &= 1 - \frac{\alpha(0)}{3\pi} \sum_i Q_i^2 \ln \frac{M^2}{m_i^2} \Theta(M^2 - m_i^2) < 1 \quad . \end{aligned} \quad (3.5)$$

Finally, we may combine (3.1) with (3.3) to yield

$$M_Z^2 = \left(\frac{\alpha(0) \pi}{\sqrt{2} G_\mu} \right) \frac{1}{s_W^2 c_W^2 (1 - \Delta r)} \quad . \quad (3.6)$$

This equation may now be used in conjunction with (3.4) and (3.5) to predict s_W^2 in terms of G_μ , $\alpha(0)$ and M_Z^2 , keeping the presently unknown mass of the top quark, m_t , as a free parameter. The W mass is obtained subsequently from (3.1).

The radiative corrections given by (3.4) have two different sources. There is first of all the contribution of the light leptons and quarks which, according to (3.5), leads to $\alpha(0)/\alpha(M^2) < 1$. Secondly, there is the additional contribution of the heavy top quark, which tends to increase $1 - \Delta r$ towards $1 - \Delta r \approx 1$. It contains the well-known dominant term⁹⁾ proportional to m_t^2 which may be traced back to the SU(2) breaking effect induced by $m_t > M_W \gg m_b$ in the masses of the charged and neutral unmixed vector bosons in (A4) and (A20). We emphasize the additional logarithmic correction in (3.4) which is due to the corrections of the tree-level relations in (2.22) and (2.24) and becomes important for $m_t \gtrsim 130$ GeV.

For the numerical evaluation we put $G_\mu = 1.16634 \cdot 10^{-5} \text{ GeV}^{-2}$ and $\alpha^{-1} = 137.035963$ and choose

$$\begin{aligned} m_u &= m_d = 0.1 \text{ GeV} \quad , \\ m_s &= 0.3 \text{ GeV} \quad , \\ m_c &= 1.5 \text{ GeV} \quad , \\ m_b &= 4.5 \text{ GeV} \end{aligned} \quad (3.7)$$

for the quark masses to be used in (3.5). These values are consistent^{22,23)} with the various thresholds in $e^+e^- \rightarrow \text{hadrons}$ and coincide with the masses chosen in the recent analysis of Ref. 24. From (3.5) one obtains

$$\alpha(M^2)^{-1} = 128 \quad (3.8)$$

for $M = M_Z$ and $m_t > M_W$.

Our results for M_W and s_W^2 for various choices of m_t and M_Z are presented in Table 1 and compared with the numerical results of a complete one-loop calculation by Lynn and Stuart¹⁴⁾ for the particular value of the Higgs boson mass of $m_H = 100$ GeV. As seen in Table 1, the agreement of the two predictions is very good. The difference between the two calculations varies between 10 MeV and 90 MeV in the prediction of M_W , corresponding to a difference in s_W^2 between 0.0003 and 0.0019. We have also compared our results with the results of a complete one-loop calculation¹⁵⁾ by Jegerlehner and find that our values of M_W never differ from

his results for M_W (for $m_H = 100$ GeV) by more than 110 MeV. Jegerlehner also gives the expected errors in his predictions due to uncertainties in the experimental data for $e^+e^- \rightarrow$ hadrons used as input and an estimate of the errors induced by the neglect of higher-order corrections. We find that our results for M_W agree with his results within twice his estimated error.

As expected, the discrepancy between our dominant fermion-loop calculation and the full one-loop calculation becomes larger when m_H is increased from $m_H = 100$ GeV to $m_H = 1$ TeV. The increase of Δr with increasing m_H implies an increase of s_W^2 according to (3.6) and a corresponding decrease of M_W . The discrepancy between our results and the complete one-loop calculation^{14,15)} reaches about 250 MeV for a choice of the Higgs mass of $m_H \cong 1$ TeV.

In Fig. 2 we compare for $M_Z = 93$ GeV our results for Δr as a function of m_t with the results²⁵⁾ of a complete one-loop calculation for various choices of m_H . For $m_H = 100$ GeV the discrepancy between our results and the full one-loop calculation is always less than 7%. For, e.g., $m_t = 45$ GeV we obtain

$$\Delta r = 0.0676 \quad , \quad (3.9)$$

which deviates by 5% from the result

$$\Delta r = 0.0713 \pm 0.0013 \quad (3.10)$$

of a complete one-loop calculation^{15,16)} for $m_H = 100$ GeV.

Relations (3.4) and (3.6) may also be used to derive an upper limit on the top quark mass, m_t , by inserting the Z mass obtained in the UA1 and UA2 experiments^{26,17)}

$$M_Z = (91.9 \pm 1.8) \text{ GeV} \quad (3.11)$$

and the average value of^{16,24)}

$$s_W^2 = 0.233 \pm 0.003 \pm 0.005 \quad (3.12)$$

from deep inelastic neutrino scattering. Due to the proximity of our results for Δr and s_W^2 to the results of the full one-loop calculation, our result of

$$m_t \lesssim 180 \text{ GeV} \quad (3.13)$$

agrees with the result obtained¹⁷⁾ by Langacker, Marciano and Sirlin.

The exceedingly small discrepancy of Table 1 between our calculation based on the dominant fermion loops and the complete one-loop calculation is not an unexpected one. Corrections to our calculation are first of all due to the neglected

contributions of the light fermions of order α/π , or at most of order $\alpha_W/\pi \approx 4\alpha/\pi$, not enhanced by large logarithms. Secondly, there are loop contributions involving bosons. For a Higgs boson mass of $m_H \approx M_W \approx M_Z \approx 100$ GeV which acts as an effective cut-off for the boson loops, we expect also these contributions to be of the order α/π . We thus expect a discrepancy between our results and the complete one-loop calculations with $m_H = 100$ GeV of the order of

$$\Delta M_W = \frac{\Delta M_W^2}{2M_W} = \frac{\alpha}{2\pi} M_W \approx 95 \text{ MeV} \quad (3.14)$$

and

$$\Delta s_W^2 = -\frac{\Delta M_W^2}{M_Z^2} = -2c_W^2 \frac{\Delta M_W}{M_W} \approx -0.0019 \quad (3.15)$$

These estimates agree with the largest discrepancies found in the direct comparison of Table 1. The results of Table 1 in fact support the hypothesis that the neglected contributions are of the order of α/π rather than of the order of α_W/π .

We end this Section with a few comments on the significance of the results on the radiative corrections in the dominant fermion-loop approximation. While the validity of the $SU(2)_L \times U(1)_Y$ spontaneously broken electroweak theory has been implicitly assumed, it must be emphasized that the fermion-loop corrections actually only depend on the structure and magnitude of the couplings of the vector bosons to the leptons and quarks. It is true that these couplings arise as a consequence of the spontaneously broken $SU(2)_L \times U(1)_Y$ gauge theory, but an equally credible derivation of the interactions of the vector bosons with the leptons and quarks is obtained^{19,20)} within the framework of a globally $SU(2)_{WI}$ weak isospin invariant massive vector boson theory broken by the photon via the W-dominance substitution rule $W_\mu^3 \rightarrow W_\mu^3 + \lambda A_\mu$ with* $\lambda = e/g_W$. In other words, the fermion-loop corrections are evidently completely independent of the Higgs sector of the theory or, more generally, the mass generating mechanism, and they are equally independent of the vector-boson self-interactions implied by the non-Abelian gauge principle.

Corrections of or deviations from the predictions of the radiative corrections in the dominant fermion-loop approximation strongly depend on the mass of the Higgs boson. Additional corrections arise, e.g., from the possible existence of

* This condition is a necessary consequence of the substitution rule $W_\mu^3 \rightarrow W_\mu^3 + \lambda A_\mu$.

supersymmetric particles and/or the existence of additional vector bosons which are expected to be present, e.g., within composite models and within superstring motivated extended gauge theories. By comparing sufficiently accurate experimental results for M_W and/or s_W^2 with the predictions of the dominant fermion-loop calculations one will be able, at least in principle, to establish the existence of additional radiative effects or put a bound on their magnitude.

As for the accuracy in the measurements of M_W and s_W^2 which will be desirable, one may be guided by the discrepancies between the dominant fermion-loop and the full one-loop calculations shown in Table 1 and Fig. 2, keeping in mind that an increase of m_H from $m_H \cong 100$ GeV to $m_H \cong 1$ TeV will increase the discrepancy in M_W (s_W^2) from $\Delta M_W \cong 50$ MeV (-0.001) to $\Delta M_W \cong 250$ MeV (-0.005). From Table 1 and Fig. 2 one concludes that within the unmodified $SU(2)_L \times U(1)_Y$ theory, even the most precise measurement^{27,28)} of s_W^2 using polarized e^\pm beams at LEP and aiming at an accuracy of $\Delta s_W \cong 0.0004$ (corresponding to $\Delta M_W \cong 20$ MeV) might barely be able to establish a discrepancy from the dominant fermion-loop results. We hasten to add that this conclusion only holds for $m_H \cong 100$ GeV, and if none of the above mentioned "new physics" phenomena are realized in nature. A heavy Higgs boson and other "new physics" phenomena may in fact lead to significant deviations in the experimental results from the calculation in the dominant fermion-loop approximation shown in Table 1 and Fig. 2.

4. Radiative Corrections to Neutrino Scattering

In this Section we consider the radiative corrections* to be applied when extracting the weak angle, s_W^2 , from measurements of neutrino hadron and neutrino lepton scattering. We will show that the dominant fermion-loop correction of Section 2 is sufficient to calculate the radiative corrections to s_W^2 with an accuracy of the order of $\alpha/\pi = 0.002$, provided the well-known QED correction to charged current interactions of neutrinos with quarks and the neutrino charge radius correction in neutral current interactions are taken into account in addition to the fermion-loop corrections to the propagator.

The basic effective Hamiltonian for calculating neutrino scattering processes with the inclusion of the dominant radiative corrections is given by

$$\begin{aligned}
 H = & \frac{G_\mu}{\sqrt{2}} [\bar{\nu}_\mu \gamma^\lambda (1 - \gamma_5) \mu \bar{e} \gamma_\lambda (1 - \gamma_5) \nu_e + \text{h.c.}] \\
 & + (1 + \frac{\alpha(M^2)}{2\pi} \ln \frac{M^2}{v^2}) (\bar{\nu}_\mu \gamma^\lambda (1 - \gamma_5) \mu \bar{u} \gamma_\lambda (1 - \gamma_5) u + \text{h.c.}) \\
 & + 2\rho \bar{\nu}_\mu \gamma^\lambda (1 - \gamma_5) \nu_\mu (j_{L\lambda}^{(3)} - \hat{s}_W^2(q^2) j_\lambda^{\text{em}}) \quad . \quad (4.1)
 \end{aligned}$$

This Hamiltonian corresponds to the diagrams in Fig. 3. It contains the charged current neutrino lepton interaction, the charged current interaction of neutrinos with u and d quarks and the neutral current interaction with leptons and quarks. The normalization of the charged current neutrino lepton interaction is an immediate consequence of relation (2.12). The normalization factor is identical to G_μ even when fermion-loop corrections to the propagator are taken into account. The charged current interaction of neutrinos with quarks contains⁸⁾ the additional well-known QED correction originating from the diagrams of Fig. 3c,

$$f = 1 + \frac{\alpha(M^2)}{2\pi} \ln \frac{M^2}{v^2} \quad , \quad (4.2)$$

where $v^2 = \max(|q^2|, m_\mu^2)$ with q^2 denoting the neutrino momentum transfer in the scattering process. Finally, the normalization of the neutral current interaction in (4.1) is due to (2.38) and contains the correction factor ρ given by

* Compare refs. 29 and 30 for calculations of the radiative corrections to be applied in the case of neutrino hadron scattering and ref. 23 for the case of $\nu_\mu (\bar{\nu}_\mu)$ electron scattering. The dependence of the radiative corrections on m_t has recently been studied in refs. 31 to 33.

(2.42). For $m_t > M_W$ we have $\rho > 1$. The effective weak angle, $\hat{s}_W^2(q^2)$, in (4.1) is given by

$$\hat{s}_W^2(q^2) = \bar{s}_W^2(q^2) - \frac{\alpha(q^2)}{6\pi\rho} \ln \frac{M^2}{v^2} \quad . \quad (4.3)$$

The first term, $\bar{s}_W^2(q^2)$, is due to the effect of fermion-loop corrections to the Z boson propagator. According to (2.33) and (2.28), $\bar{s}_W^2(q^2)$ is related to $s_W^2 \equiv 1 - M_W^2/M_Z^2$ via

$$\bar{s}_W^2(q^2) = \frac{\alpha(q^2)}{\alpha(M^2)} (s_W^2 + (1-s_W^2) \delta\bar{\rho} - \alpha(M^2) b_2 A(q^2)) \quad , \quad (4.4)$$

where, according to (2.29) and (2.41), the parameter $\bar{\rho}$ differs from ρ by an additional correction term which depends logarithmically on the top quark mass, m_t , and $b_2 A(q^2)$ is given by (2.40). From the second equality in (2.33) we know that $\bar{s}_W^2(q^2) = \alpha(q^2) / \alpha_W(q^2)$ for $m_t < M_W$, i.e., $\bar{s}_W^2(q^2)$ is in general less strongly dependent on q^2 than $\alpha(q^2)$ or $\alpha_W(q^2)$. The second term in (4.3) is of completely different origin from the first one. It is due to the neutrino charge radius contribution (shown in Fig. 3b) which is due to photon exchange and charged current weak interactions and is thus completely unrelated to the neutral current interactions induced by Z boson exchange. The possibility of this contribution which is invariant by itself under gauge transformations in the leading log approximation was pointed out³⁴⁾ as early as 1963 by Bernstein and Lee. We finally note that our expression (4.1) for the effective Hamiltonian is very similar to the one given⁶⁾ by Antonelli and Majani. It is different insofar as we have included the possibility of a very massive top quark and also discriminate clearly between $\hat{s}_W^2(q^2)$ and $\bar{s}_W^2(q^2)$.

The weak angle in neutrino scattering is deduced from the measurements of the ratio of the neutral to charged current cross-sections by neutrinos

$$R_\nu = \frac{\sigma(\nu_\mu N \rightarrow \nu_\mu X)}{\sigma(\nu_\mu N \rightarrow \mu^- X)} \quad (4.5)$$

or antineutrinos

$$R_{\bar{\nu}} = \frac{\sigma(\bar{\nu}_\mu N \rightarrow \bar{\nu}_\mu X)}{\sigma(\bar{\nu}_\mu N \rightarrow \mu^+ X)} \quad (4.6)$$

and from the Paschos-Wolfenstein quantities³⁵⁾

$$R^\pm = \frac{\sigma(\nu_\mu N \rightarrow \nu_\mu X) \pm \sigma(\bar{\nu}_\mu N \rightarrow \bar{\nu}_\mu X)}{\sigma(\nu_\mu N \rightarrow \mu^- X) \pm \sigma(\bar{\nu}_\mu N \rightarrow \mu^+ X)} \quad , \quad (4.7)$$

where N denotes an isoscalar target. In terms of the empirically determined $\nu/\bar{\nu}$ ratio

$$r = \frac{\sigma(\nu_{\mu} N \rightarrow \mu^{-} X)}{\sigma(\bar{\nu}_{\mu} N \rightarrow \mu^{+} X)} \quad (4.8)$$

which is introduced in order to minimize theoretical uncertainties due to strong interactions³⁰⁾, the measured ratios R_{ν} , $R_{\bar{\nu}}$ and R^{\pm} determine the weak angle $\hat{s}_W^2(q^2)$ in (4.1) via

$$R = \left(\frac{O}{F}\right)^2 \left(B(r) \hat{s}_W^4(q^2) - \hat{s}_W^2(q^2) + \frac{1}{2} \right) \quad , \quad (4.9)$$

where³⁰⁾

$$B(r) = \left. \begin{array}{l} \frac{5}{9} (1+r) \\ \frac{5}{9} (1+1/r) \\ \frac{10}{9} \\ 0 \end{array} \right\} \text{ for } \left\{ \begin{array}{l} R_{\nu} \\ R_{\bar{\nu}} \\ R^{+} \\ R^{-} \end{array} \right. \quad . \quad (4.10)$$

In arriving at (4.9) one assumes that the structure function of an isoscalar nucleus consists of u, d and \bar{u} and \bar{d} quarks only and one neglects the Cabibbo angle.

From R one deduces the effective weak angle $\hat{s}_W^2(q^2)$ for the value of q^2 at which ν -scattering is measured, and one finally obtains s_W^2 by using (4.3) and (4.4). This radiatively corrected value differs from s_B^2 , the value of the weak angle obtained by using the Born approximation when evaluating the experimental data, i.e.,

$$R = B(r) s_B^4 - s_B^2 + \frac{1}{2} \quad , \quad (4.11)$$

by the amount

$$(\delta s_W^2)_{RC} \equiv s_W^2 - s_B^2 \quad , \quad (4.12)$$

which is the radiative correction we wish to determine from the effective Hamiltonian (4.1).

From (4.9) and (4.11) we find in lowest order in α^8)

$$\hat{s}_W^2(q^2) - s_B^2 = \frac{2(f - \rho) R}{(2B s_B^2 - 1)} \quad . \quad (4.13)$$

Substituting (4.3) and (4.4) in (4.13) and noting that in the expression for

$s_W^2 - s_B^2$ obtained upon substitution, s_B^2 may be replaced by s_W^2 in first order in α , we arrive at the simple formula

$$(\delta s_W^2)_{RC} = \alpha(M^2) \left[\frac{1}{6\pi} \ln \left(\frac{M^2}{|q^2|} \right) + b_2 A(q^2) + \left(\frac{1}{\alpha(q^2)} - \frac{1}{\alpha(M^2)} \right) s_W^2 \right] \\ + \frac{2B(r) s_W^4 - 2s_W^2 + 1}{1 - 2B(r) s_W^2} (\rho - f) - (1 - s_W^2) (\bar{\rho} - 1) \quad . \quad (4.14)$$

For typical SPS (CERN) or FNAL neutrino experiments we have $\langle |q^2| \rangle = 20 \text{ GeV}^2$, implying that $b_2 A(q^2)$ from (2.40) becomes

$$b_2 A(|q^2| \cong 20 \text{ GeV}^2) = \frac{1}{12\pi} \left[\ln \left(\frac{|q^2|^{1/2} m_b^2}{M_Z^2} \right) + 2 \ln \left(\frac{m_t^2}{M_Z^2} \right) \Theta(M - m_t) \right] , \quad (4.15)$$

while $\alpha(q^2)$ and $\alpha(M^2)$ are deduced from (2.32) and (2.40) and ρ , $\bar{\rho}$ and f are given by (2.41), (2.42) and (4.2).

When evaluating (4.14) we use the CDHS result³⁶⁾ of $r = 0.39$ and the CHARM result³⁷⁾ of $r = 0.456$ and calculate the radiative correction, $(\delta s_W^2)_{RC}$, for the CDHS and CHARM experiments. Using as input $M_Z = 91.8 \text{ GeV}$ and $m_t = 45 \text{ GeV}$ yields $s_W^2 = 0.2295$ from (3.6). Inserting this value and $M \cong M_Z$ in (4.14) one obtains

$$(\delta s_W^2)_{RC} = -0.0098 \quad (\text{CDHS}) \quad , \\ (\delta s_W^2)_{RC} = -0.0101 \quad (\text{CHARM}) \quad , \quad (4.16)$$

These results are in excellent agreement with the results quoted by the experimental groups on the basis of a complete one-loop calculation for the same value of $m_t = 45 \text{ GeV}$ and $m_H = 100 \text{ GeV}$,

$$(\delta s_W^2)_{RC} = -0.011 \pm 0.002 \quad (\text{CDHS}) \quad , \\ (\delta s_W^2)_{RC} = -0.0092 \pm 0.002 \quad (\text{CHARM}) \quad . \quad (4.17)$$

To proceed further we give in Table 2 the radiative corrections, $(\delta s_W^2)_{RC}$ as a function of m_t for experiments measuring R_ν , R^+ and R^- . We again use $M_Z = 91.8 \text{ GeV}$ as input and vary m_t . The corresponding values of s_W^2 are given in Table 2, as well as the results for $(\delta s_W^2)_{RC}$. The results for the case of R_ν are compared with the results of the full one-loop calculations of Bardin and Dokuchaeva³¹⁾ which are based on $m_H = 100 \text{ GeV}$. We see that the discrepancy between our results for $(\delta s_W^2)_{RC}$ in experiments measuring R_ν and those of Ref. 29 is always less than 0.002. A similar conclusion is also reached when we compare our results with those of Stuart³²⁾.

We also note that the radiative correction to R according to Table 2 is insensitive to the value of m_t . Our results on the dependence of $(\delta s_W^2)_{RC}$ on m_t in Table 2 are essentially in agreement within an error of the order of $\alpha/\pi \approx 0.002$ with a recent study³³⁾ by Sirlin using a complete one-loop calculation.

We now turn to the radiative corrections to be applied when extracting s_W^2 from measurements of the $\nu_\mu e/\bar{\nu}_\mu e$ ratio. In the Born approximation we now have

$$R_{\nu e} = \frac{\sigma(\nu_\mu e \rightarrow \nu_\mu e)}{\sigma(\bar{\nu}_\mu e \rightarrow \bar{\nu}_\mu e)} = \frac{16s_B^4 - 12s_B^2 + 3}{16s_B^4 - 4s_B^2 + 1} \quad , \quad (4.18)$$

and the radiative corrections from the Hamiltonian (4.1) are obtained as

$$\begin{aligned} (\delta s_W^2)_{RC} = & \alpha(M^2) \left[\frac{1}{6\pi} \ln \left(\frac{M^2}{|q^2|} \right) + b_2 A(q^2) + \right. \\ & \left. + \left(\frac{1}{\alpha(q^2)} - \frac{1}{\alpha(M^2)} \right) s_W^2 \right] - (1 - s_W^2) (\bar{\rho} - 1) \quad . \quad (4.19) \end{aligned}$$

Substituting $b_2 A(q^2)$ from (2.40) and evaluating (4.19) for $\langle |q^2| \rangle = (0.3 \text{ GeV})^2$ we again obtain $(\delta s_W^2)_{RC}$ for various values of m_t as shown in Table 2. The results of Table 2 are again in agreement with the full one-loop calculation³³⁾ by Sirlin.

In summary, the simple and compact formulae (4.14) and (4.19) based on the notion of "running coupling constants" and the dominant fermion-loop approximation, supplemented by the charged current QED and the neutrino charge radius correction, yield the radiative corrections to be applied to s_B^2 to an excellent approximation. Needless to say, the significance of neutrino scattering experiments as a test of the $SU(2)_L \times U(1)_Y$ theory lies in establishing a consistency (or inconsistency) of the radiatively corrected values of s_W^2 with the results for s_W^2 calculated from G_μ , α and M_Z and the results calculated from the ratio of M_W and M_Z .

5. Summarizing Conclusion: The Strategy for Future Precision Tests of the Electroweak Theory

The spirit of the present investigation is best characterized by quoting Feynman³⁸⁾: "In any event, it is always a good idea to try to see how much or how little of our theoretical knowledge actually goes into the analysis of those situations which have been experimentally checked" - or will be experimentally checked in the future, as we may add within the present context.

The analysis of the present paper shows how strongly fermion-loop corrections to the propagators dominate the radiative corrections to the electroweak parameters. While the dominating role of the fermion loops has been qualitatively known for a long time, a thorough quantitative analysis including the case of a very massive top quark, $m_t > M_W$, and leading to comparative Tables and Figures has, to the best of our knowledge, not been carried out as yet. For $m_H \approx 100$ GeV (compare Table 1), the discrepancy in the prediction of M_W from α , G_μ and M_Z between the present calculation and the complete one-loop results ranges from a few times 10 MeV to 100 MeV, depending on the value of m_t . This is in agreement with the error in the calculation which is estimated to be of the order of $(\alpha/2\pi) M_W \approx 100$ MeV or, equivalently, $\Delta s_W^2 \approx 0.002$. For $m_H \approx 1$ TeV, the discrepancy between the dominant fermion-loop approximation and the complete one-loop results may increase to about 250 MeV, while for $m_H \gg 1$ TeV the perturbative boson-loop calculations become unreliable. These figures set the scale for the accuracy needed if future measurements are to test the theory beyond the dominant fermion-loop approximation.

Apart from providing an excellent approximation to the full one-loop calculation, the dominant fermion-loop approximation leads to an exceedingly simple and intuitively satisfactory picture of the radiative corrections in terms of q^2 -dependent ("running") coupling constants and vector boson masses. Two cases, $m_t < M_W$ and $m_t > M_W$ have to be discriminated. For $m_t < M_W$ the radiative effects may be summarized by noting that the Fermi coupling, G_μ , is independent of q^2 ("does not run") and all tree-level relations between masses and couplings remain intact for the q^2 -dependent quantities. Care must be taken when deducing the weak angle, s_W^2 , from neutrino scattering, where additional photon exchange corrections have to be taken into account. If $s_W^2 \equiv 1 - M_W^2/M_Z^2$ is used in the mass formulae, the radiative correction is exclusively determined by the ratio of $\alpha(0)/\alpha(M^2) < 1$, which is unequal to 1 due to the q^2 dependence of $\alpha(q^2)$. For $m_t > M_W$ an additional and possibly large mass scale, m_t , enters the calculation and

leads to important additional terms in the various relations for the q^2 -dependent quantities. In particular, the deviation of the $\bar{\rho}$ parameter from $\bar{\rho} = 1$ induces additional corrections which are quadratic and logarithmic in m_t and tend to decrease the quantity Δr determining the radiative corrections to the vector boson masses from $\Delta r \approx 0.07$ to $\Delta r \approx 0$, if the extreme value of $m_t \approx 200$ GeV is chosen.

The main conclusion of the present paper, a strategy for future precision tests of the electroweak theory, now follows immediately. Discriminating clearly the radiative effects induced by the empirically tested vector boson fermion interactions from the "new physics" of the vector boson self-interactions and possibly other new phenomena, e.g., the effects of a strongly interacting Higgs sector, of compositeness, etc., it seems highly suggestive in the analysis of future precision data to start from a comparison of these data with the predictions of the dominant fermion-loop approximation. Both disagreement of the data with these predictions or agreement within errors will strongly constrain the bosonic sector of the theory as well as other new phenomena (whereby m_t is assumed to be known), and it might teach us something about the physics at the energy scale of 1 or 2 TeV. In fact, it seems to us that the proposed procedure for analysing future precision data on M_W , M_Z and s_W^2 gives us the only chance to see, to isolate and to test directly the radiative effects due to the bosonic sector, i.e., due to that part of the theory which is uniquely related to the celebrated renormalizability properties³⁹⁾ of the spontaneously broken electro-weak gauge theory⁴⁾.

Appendix A: The Renormalization of the W^\pm and γZ Propagators

In this Appendix we will give a brief derivation of the expressions (2.2) and (2.14) for the renormalized propagators of the W^\pm and the γZ system which include the vacuum polarization effects due to the lepton and quark loops shown in Figs. 1a,b. We will include three families of leptons and quarks. The generalization to more than three families is a simple task. All leptons and quarks with the exception of the possibly very massive top quark are treated as massless. As for the mass of the top quark, we will explicitly discriminate between the two cases of $m_t < M_W$ (the "massless" case) and $m_t > M_W$ (the very massive case).

The renormalization of the W^\pm propagator is straightforward. In lowest order of perturbation theory the transverse part of the W^\pm propagator is given by

$$-i(\Delta_0^W)^{-1}_{\mu\nu} = T_{\mu\nu} (q^2 - M_W^{(0)2}) \quad , \quad (A1)$$

where

$$T_{\mu\nu} = g_{\mu\nu} - \frac{q_\mu q_\nu}{q^2} \quad . \quad (A2)$$

Introducing the modification due to lepton and quark loops (Fig. 1a) one obtains

$$-i(\Delta_0^W)^{-1}_{\mu\nu} = T_{\mu\nu} [q^2(Z_W^{-1} + \Pi_W^{(0)}(q^2)) - \tilde{M}_W^{(0)2}] \quad (A3)$$

where

$$\tilde{M}_W^{(0)2} = \begin{cases} M_W^{(0)2} & \text{for } m_t < M_W \quad , \\ M_W^{(0)2} + m_t^2 t_W^{(0)} & \text{for } m_t > M_W \quad . \end{cases} \quad (A4)$$

In (A3) we have kept the notation of (A1) for the propagator. The index 0 now denotes unrenormalized quantities. The contribution of a very massive top quark, $m_t > M_W$, in (A4) is due to the quadratically divergent part of the quark loop and is given by

$$m_t^2 t_W^{(0)} = m_t^2 \frac{3\alpha_W^{(0)}}{8\pi} \left(\ln \frac{\Lambda^2}{m_t^2} + \frac{1}{2} \right) \quad . \quad (A5)$$

Keeping the leading logarithms for the light leptons and quarks, the vacuum polarization function in (A3) becomes

$$\Pi_W^{(0)}(q^2) = -\frac{\alpha_W^{(0)}}{3\pi} b_1 \ln\left(-\frac{q^2}{M^2}\right) \quad , \quad (A6)$$

and the (ultra-violet-divergent) renormalization constant, Z_W^{-1} , is found to be

$$Z_W^{-1} = 1 + \begin{cases} \frac{\alpha_W^{(0)}}{3\pi} \frac{n}{4} \ln \frac{\Delta^2}{M^2} & \text{for } m_t < M_W \\ \frac{\alpha_W^{(0)}}{3\pi} \left(\frac{n}{4} \ln \frac{\Delta^2}{M^2} + \frac{3}{4} \ln \frac{M^2}{m_t^2} \right) & \text{for } m_t > M_W \end{cases} \quad (A7)$$

The constant b_1^i is defined by (2.7) and is given by

$$b_1^i = \begin{cases} \frac{n}{4} = \frac{12}{4} = 3 & \text{for } m_t < M_W \\ \frac{9}{4} & \text{for } m_t > M_W \end{cases} \quad (A8)$$

In (A6) and (A7) the unrenormalized coupling of the W^\pm to the leptons and quarks is denoted by $\alpha_W^{(0)} = g_W^{(0)}/4\pi$ and the ultra-violet cut-off by Δ . The sum of Z_W^{-1} and $\Pi_W^{(0)}(q^2)$ in (A3) is independent of the renormalization scale, M , which is to be identified with the empirically observed mass of the W^\pm , i.e.,

$$M = M_W \quad (A9)$$

Multiplying the propagator (A3) by the coupling, $\alpha_W^{(0)}$, to the outgoing leptons and quarks in Fig. 1a and introducing the renormalized W^\pm mass,

$$M_W^2 = \begin{cases} Z_W M_W^{(0)2} & \text{for } m_t < M_W \\ Z_W (M_W^{(0)2} + m_t^2 t_W^{(0)}) & \text{for } m_t > M_W \end{cases} \quad (A10)$$

as well as the renormalized coupling constant at the mass scale $M = M_W$,

$$\alpha_W(M_W^2) = \frac{g_W^2(M_W)}{4\pi} = Z_W \alpha_W^{(0)} \quad (A11)$$

(A3) may be rewritten in the form of (2.2) in the main text, i.e.,

$$i(\Delta_0^W)_{\mu\nu} \alpha_W^{(0)} = T_{\mu\nu} \frac{\alpha_W(M_W^2)}{q^2(1 + \Pi_W(q^2)) - M_W^2} = \alpha_W(M^2) (\Delta^W)_{\mu\nu} \quad (A12)$$

Here, $(\Delta^W)_{\mu\nu}$ denotes the renormalized propagator,

$$(\Delta^W)_{\mu\nu} = Z_W^{-1} (\Delta_0^W)_{\mu\nu} \quad (A13)$$

or, equivalently (compare with the γZ propagator renormalization, (A29))

$$(\Delta^W)^{-1} = \sqrt{Z_W} (\Delta_0^W)^{-1} \sqrt{Z_W} \quad (A13a)$$

and $\Pi_W(q^2)$ denotes the renormalized vacuum polarization

$$\Pi_W(q^2) = Z_W \Pi_W^{(0)}(q^2) = - \frac{\alpha_W(M^2)}{3\pi} b_1^i \ln\left(-\frac{q^2}{M^2}\right) \quad (A14)$$

The choice (A9) of the renormalization scale assures that

$$\text{Re } \Pi_W(M_W^2) = 0 \quad , \quad (\text{A15})$$

and, consequently the zero of the real part of the inverse propagator in (A12) coincides with the empirically observed mass of the W^\pm boson.

We turn to the renormalization of the γZ propagator. Its structure is completely analogous to (A3),

$$-i(\Delta_0^{\gamma Z})_{\mu\nu}^{-1} = T_{\mu\nu}(q^2(Z^{-1} + \Pi_{\gamma Z}^{(0)}(q^2)) - M_{\gamma Z}^{(0)2}) \quad , \quad (\text{A16})$$

but in the present case, Z^{-1} , $\Pi_{\gamma Z}^{(0)}(q^2)$ and $M_{\gamma Z}^{(0)2}$ are two-by-two matrices given by

$$Z^{-1} = \begin{pmatrix} Z_Y^{-1} & \frac{s_W^{(0)}}{c_W^{(0)}} (Z_{W2}^{-1} - Z_Y^{-1}) \\ \frac{s_W^{(0)}}{c_W^{(0)}} (Z_{W2}^{-1} - Z_Y^{-1}) & \frac{s_W^{(0)2}}{c_W^{(0)2}} (Z_Y^{-1} - 2Z_{W2}^{-1}) + \frac{1}{c_W^{(0)2}} Z_{W1}^{-1} \end{pmatrix} \quad , \quad (\text{A17})$$

$$\Pi_{\gamma Z}^{(0)}(q^2) = -\frac{\alpha^{(0)}}{3\pi} \ln\left(\frac{-q^2}{M^2}\right) \begin{pmatrix} b_Q & \frac{b_2 - s_W^{(0)2} b_Q}{s_W^{(0)} c_W^{(0)}} \\ \frac{b_2 - s_W^{(0)2} b_Q}{s_W^{(0)} c_W^{(0)}} & \frac{b_2 + s_W^{(0)4} b_Q - 2s_W^{(0)2} b_2}{s_W^{(0)2} c_W^{(0)2}} \end{pmatrix} \quad (\text{A18})$$

and

$$M_{\gamma Z}^{(0)2} = \begin{pmatrix} 0 & 0 \\ 0 & \tilde{M}_Z^{(0)2} \end{pmatrix} \quad (\text{A19})$$

with

$$\tilde{M}_Z^{(0)2} = \begin{cases} \frac{M_W^{(0)2}}{c_W^{(0)2}} & \text{for } m_t < M_W \\ \frac{1}{c_W^{(0)2}} (M_W^{(0)2} + m_t^2 t_W^{(0)} - \frac{3\alpha_W^{(0)}}{16\pi} m_t^2) & \text{for } m_t > M_W \end{cases} \quad . \quad (\text{A20})$$

We note that the additive mass correction proportional to m_t^2 in (A20) is different from the correction applied in the case of the charged boson in (A4). The consequences of this additional contribution will become apparent below.

The propagator (A16) is to be used in conjunction with the current doublet

$$j_{\mu}^{(0)} = \begin{pmatrix} e^{(0)} j_{\mu}^{\text{em}} \\ \frac{e^{(0)}}{s_W^{(0)} c_W^{(0)}} (j_{L\mu}^{(3)} - s_W^{(0)2} j_{\mu}^{\text{em}}) \end{pmatrix} \quad (\text{A21})$$

containing the electromagnetic and the weak neutral current. The unrenormalized Weinberg angle is denoted by

$$s_W^{(0)} = \frac{\alpha^{(0)}}{\alpha_W^{(0)}} \quad , \quad c_W^{(0)2} = 1 - s_W^{(0)2} \quad , \quad (\text{A22})$$

where $\alpha^{(0)} = e^{(0)2}/4\pi$ is the unrenormalized electromagnetic fine-structure constant.

For $m_t > M_W$ the ultra-violet divergent renormalization parameters Z_Y , Z_{W1} and Z_{W2} in (A16) have the form

$$Z_Y^{-1} = 1 + \frac{\alpha^{(0)}}{3\pi} \tilde{b}_Q \ln \frac{\Lambda^2}{M^2} - \frac{4\alpha^{(0)}}{9\pi} \ln \frac{m_t^2}{M^2} \quad , \quad (\text{A23})$$

and

$$Z_{W1}^{-1} = Z_W^{-1} \left(1 + \frac{\alpha_W(M)}{8\pi} \ln \frac{m_t^2}{M^2} \right) \quad ,$$

$$Z_{W2}^{-1} = Z_W^{-1} \left(1 + \frac{\alpha_W}{12\pi} \ln \frac{m_t^2}{M^2} \right) \quad . \quad (\text{A24})$$

For $m_t < M_W$ the terms proportional to $\ln(m_t^2/M^2)$ have to be dropped and Z_{W1} and Z_{W2} become equal. The parameters b_1 , b_2 and b_Q depend on the weak isospin and charges of the leptons and quarks and are defined by (2.20), while \tilde{b}_Q is given by

$$\tilde{b}_Q = \sum_{\text{all fermions}} Q_i^2 = \frac{24}{3} \quad , \quad (\text{A25})$$

where the sum runs over all leptons and quarks independently of the magnitude of m_t . Finally, the choice of the renormalization scale*

* Due to the logarithmic dependence on M the difference between M_Z and M_W induces terms of the order of $\alpha \ln(M_Z/M_W)$ which are of the same order of magnitude as the terms we have neglected consistently.

$$M^2 \cong M_W^2 \cong M_Z^2 \quad (\text{A26})$$

assures that

$$\text{Re } \Pi_{YZ}^{(0)}(M_Z^2) = 0 \quad (\text{A27})$$

implying that the real part of the propagator has a pole at the empirically determined Z mass, M_Z .

The renormalization of the γZ propagator (A16) is accomplished in analogy to the case of the W propagator in (A13). Application of a suitable transformation on the propagator matrix (A16) replaces Z^{-1} by unity and $M_{YZ}^{(0)2}$ by a transformed diagonal matrix. The "renormalization transformation", ζ , is obtained by specialization of the matrix D in (B12) to the present case. Comparing the matrix Z^{-1} in (A17) with the matrix K in (B2) one finds the appropriate expressions for c_1 , c_2 and λ and subsequently, by substitution in (B12), the "renormalization matrix"

$$\zeta = \begin{pmatrix} Z_Y^{1/2} & 0 \\ \frac{s_W^{(0)}(1 - Z_Y Z_{W2}^{-1}) Z_{W1}^{1/2}}{(1 - s_W^{(0)} Z_Y Z_{W1} Z_{W2}^{-2})^{1/2}} & \frac{c_W^{(0)} Z_{W1}^{1/2}}{1 - s_W^{(0)2} Z_Y Z_{W1} Z_{W2}^{-2}} \end{pmatrix}. \quad (\text{A28})$$

By construction, application of ζ yields (compare (A13a) as well as (B13))*

$$(\Delta_{\mu\nu}^{YZ})^{-1} = \zeta (\Delta_{\mu\nu}^Z)^{-1} \zeta^t = T_{\mu\nu} [q^2(1 + \Pi_{YZ}(q^2)) - M_{YZ}^2] \quad (\text{A29})$$

where

$$\Pi_{YZ}(q^2) = \zeta \Pi_{YZ}^{(0)}(q^2) \zeta^t \quad (\text{A30})$$

and

$$M_{YZ}^2 = \zeta M_{YZ}^{(0)2} \zeta^t = \begin{pmatrix} 0 & 0 \\ 0 & M_Z^2 \end{pmatrix}, \quad (\text{A31})$$

and $\text{Re } \Pi_{YZ}(M_Z^2) = 0$ as a consequence of (A27). Explicit expressions for $\Pi_{YZ}(q^2)$ and M_{YZ}^2 will be given below.

Let us now consider the renormalized current to be used in conjunction with the renormalized propagator (A29) (compare (B14)). Applying ζ on (A21) yields

* Evidently, the transition from $(\Delta_0^{YZ})_{\mu\nu}$ to the renormalized propagator $(\Delta_{YZ}^Z)_{\mu\nu}$ corresponds to the transition from the unrenormalized to the renormalized photon and Z fields.

$$\zeta j_\mu = \begin{pmatrix} e(M^2) j_\mu^{em} \\ g_Z(M^2) (j_{L\mu}^{(3)} - \bar{s}_W^2(M^2) j_\mu^{em}) \end{pmatrix} . \quad (A32)$$

The renormalized electromagnetic coupling, $e(M^2)$, at the scale M^2 is related to the unrenormalized one which is present in (A21) via

$$\alpha(M^2) = \frac{e^2(M^2)}{4\pi} = Z_Y \frac{e^{(0)2}}{4\pi} = Z_Y \alpha^{(0)} , \quad (A33)$$

and the radiatively corrected weak angle, $\bar{s}_W(M)$, in (A32) is given by

$$\bar{s}_W^2(M^2) = s_W^{(0)} \frac{Z_Y}{Z_{W2}} = \frac{\alpha(M^2)}{\alpha_W(M^2)} \left(1 + \frac{\alpha_W(M^2)}{12\pi} \ln \frac{m_t^2}{M_W^2} \right) . \quad (A34)$$

In (A34) we used (A33) and the explicit expression for Z_{W2} given in (A24). The renormalized Z-coupling in (A32) is found to be

$$\alpha_Z(M^2) = \frac{\alpha(M^2)}{\bar{s}_W^2 \bar{c}_W^2 \left(1 + \frac{\alpha_W(M^2)}{24\pi \bar{c}_W^2} \ln \frac{m_t^2}{M^2} \right)} = \frac{\alpha_W(M^2)}{\bar{c}_W^2 \left(1 + \frac{\alpha_W(M^2)}{24\pi} \left(2 + \frac{1}{\bar{c}_W^2} \right) \ln \frac{m_t^2}{M^2} \right)} . \quad (A35)$$

According to (A34) and (A35), the tree level relations for \bar{s}_W^2 and α_Z are modified for $m_t \gg M_W$ by correction terms which depend logarithmically on m_t . These correction terms are not present for $m_t < M_W$.

We return to the renormalized propagator (A29). An explicit evaluation of (A30) shows that $\Pi_{YZ}(q^2)$ is obtained from $\Pi_{YZ}^{(0)}(q^2)$ in (A18) by making the replacement

$$s_W^{(0)} \rightarrow \bar{s}_W , \quad c_W^{(0)} \rightarrow \bar{c}_W \sqrt{d} , \quad (A36)$$

where d is given by (2.17). This replacement yields (2.15) in the main text. Finally, using (B7) one finds that the radiatively corrected Z mass in (A31) is given by

$$M_Z^2 = \frac{M_W^2}{\bar{c}_W^2} \left(1 + \frac{3\alpha_W(M^2)}{16\pi} \frac{m_t^2}{M_W^2} + \frac{\alpha_W(M^2)}{24\pi} \left(2 + \frac{1}{\bar{c}_W^2} \right) \ln \frac{m_t^2}{M_W^2} \right)^{-1} . \quad (A37)$$

The tree level relation for M_Z is thus corrected by terms which are quadratic and logarithmic in m_t (for $m_t > M_W$). Combining (A35) with (A37) one finds that the ratio α_Z/M_Z^2 receives a quadratic correction only,

$$\frac{\alpha_Z(M^2)}{M_Z^2} = \frac{\alpha_W(M^2)}{M_W^2} \left(1 + \frac{3\alpha_W(M^2)}{16\pi} \frac{m_t^2}{M_W^2} \right) . \quad (A38)$$

The factor relating α_W/M_W^2 to α_Z/M_Z^2 may be traced back to the different top quark contributions to the charged and neutral vector boson masses in (A4) and (A20). Indeed, from (A20), using the renormalization relations (A10) and (A11), we conclude that

$$\frac{\alpha_Z^{(0)}}{\tilde{M}_Z^{(0)2}} = \frac{\alpha_W}{M_W^2} \left(1 + \frac{3\alpha_W(M^2)}{16\pi} \frac{m_t^2}{M_W^2} \right) . \quad (A39)$$

Here, according to (A21) and (A22) we have

$$\alpha_Z^{(0)} = g_Z^{(0)2}/4\pi = e^{(0)2}/4\pi s_W^{(0)2} c_W^{(0)2} = \alpha_W^{(0)2}/c_W^{(0)2} . \quad (A40)$$

Relation (A38) now follows immediately by noting that α_Z is obtained from $\alpha_Z^{(0)}$ by multiplication with the same factor which relates M_Z^2 to $\tilde{M}_Z^{(0)2}$ (compare (B7) and (B14)).

Appendix B: The Diagonalization of the γZ Propagator

The fermion loop corrections to the photon and Z-boson propagators shown in Fig. 1b lead to a two by two propagator matrix containing off-diagonal elements. In this Appendix we give the formalism for the diagonalization of a propagator matrix of the general structure obtained on the basis of Fig. 1b. This diagonalization of the propagator is essential for an interpretation of the corrected propagator in terms of (renormalized) fields associated with the photon and Z-boson. The method to be used for the diagonalization of the propagator consists of a slight generalization of the procedure⁴⁰⁾ applied in Lagrangian models containing a γW^3 so-called "current mixing" term.

Suppressing Lorentz indices which are irrelevant in the present connection, the propagator $\Delta(q^2)$ to be considered has the form

$$\Delta(q^2) = (q^2 K - M^2)^{-1} \quad , \quad (B1)$$

where

$$K = \begin{pmatrix} c_1 & \lambda \\ \lambda & c_2 \end{pmatrix} \quad (B2)$$

and

$$M^2 = \begin{pmatrix} 0 & 0 \\ 0 & m^2 \end{pmatrix} \quad . \quad (B3)$$

The parameters c_1 , c_2 and λ may be constants (as encountered in the case of the renormalization of the propagator matrix in Appendix A) or may be dependent on q^2 (as in section 2, when one introduces q^2 dependent "running" coupling constants). The mass matrix (B3) contains a vanishing and a non-vanishing mass to be identified in the applications with the photon and Z-boson mass, respectively. In view of the applications in Appendix A and in section 2 we consider the matrix element of the propagator (B1) formed with a two-component current of the form

$$j = \begin{pmatrix} e j^{em} \\ g_Z (j^{(3)} - s_w^2 j^{em}) \end{pmatrix} \quad . \quad (B4)$$

We will now explicitly construct the transformation D which diagonalizes the propagator, i.e.,

$$j^+ \Delta(q^2) j = j^+ D^t (D^{-1})^t \Delta(q^2) D^{-1} D j = j^+ D^t \Delta_{diag}(q^2) D j \quad , \quad (B5)$$

where

$$\Delta_{\text{diag}}(q^2) = \begin{pmatrix} \frac{1}{q^2} & 0 \\ 0 & \frac{1}{q^2 - m'^2} \end{pmatrix} . \quad (\text{B6})$$

We will find that the mass m' is related to m via

$$m'^2 = \frac{m^2 c_1}{c_1 c_2 - \lambda^2} . \quad (\text{B7})$$

The transition from $\Delta(q^2)$ to $\Delta_{\text{diag}}(q^2)$ in (B5) corresponds to the transition from the original fields to appropriately chosen transformed fields which lead to vanishing off-diagonal elements in the γZ propagator.

The transformation D is found in two steps. First of all, one introduces a (non-orthogonal) transformation, D_1 , which diagonalizes the symmetric matrix K . It is given by

$$D_1 = \begin{pmatrix} \frac{1}{\sqrt{c_\Delta(1-\lambda'^2)}} & \frac{-\lambda'}{\sqrt{c_2(1-\lambda'^2)}} \\ 0 & \frac{1}{\sqrt{c_2}} \end{pmatrix} , \quad (\text{B8})$$

where

$$\lambda' = \frac{\lambda}{\sqrt{c_1 c_2}} . \quad (\text{B9})$$

One easily verifies that indeed

$$D_1 \Delta^{-1}(q^2) D_1^t = q^2 \begin{pmatrix} 1 & 0 \\ 0 & 1 \end{pmatrix} - m'^2 \begin{pmatrix} \frac{\lambda'^2}{1-\lambda'^2} & \frac{-\lambda'}{\sqrt{1-\lambda'^2}} \\ \frac{-\lambda'}{\sqrt{1-\lambda'^2}} & 1 \end{pmatrix} . \quad (\text{B10})$$

Application of the transformation D_1 thus transforms the propagator from the form (B1) which is characteristic for current mixing to the form (B10) which is characteristic for mass mixing. The diagonalization of the propagator is completed by subsequently applying the orthogonal transformation R (with $R^t = R^{-1}$),

$$R = \begin{pmatrix} \sqrt{1-\lambda'^2} & \lambda' \\ -\lambda' & \sqrt{1-\lambda'^2} \end{pmatrix} . \quad (\text{B11})$$

Application of

$$D \equiv R D_1 = \begin{pmatrix} \frac{1}{\sqrt{c_1}} & 0 \\ \frac{-\lambda}{\sqrt{c_1(c_1 c_2 - \lambda^2)}} & \frac{\sqrt{c_1}}{\sqrt{c_1 c_2 - \lambda^2}} \end{pmatrix} \quad (\text{B12})$$

fully diagonalizes the propagator. In accordance with (B5) we have

$$D \Delta^{-1}(q^2) D^t = q^2 \begin{pmatrix} 1 & 0 \\ 0 & 1 \end{pmatrix} - \begin{pmatrix} 0 & 0 \\ 0 & m'^2 \end{pmatrix} = \Delta_{\text{diag}}^{-1}(q^2) \quad , \quad (\text{B13})$$

where m'^2 is given by (B7). For the currents to be used in (B5) in conjunction with the diagonal propagator one obtains

$$Dj = \begin{pmatrix} \frac{e}{\sqrt{c_1}} j_{\text{em}} \\ g_Z \sqrt{\frac{c_1}{c_1 c_2 - \lambda^2}} (j^{(3)} - (s_w^2 + \frac{\lambda}{c_1} \frac{e}{g_Z}) j_{\text{em}}) \end{pmatrix} \quad . \quad (\text{B14})$$

It is useful to note that m^2 in (B7) and g_Z^2 in (B14) are modified by the same factor $c_1/(c_1 c_2 - \lambda^2)$.

Table 1

Comparison of the results for M_W and $s_W^2 \equiv \sin^2\theta_W$ in the dominant fermion-loop approximation of the present paper with the results of a complete one-loop calculation¹⁴⁾.

m_t (GeV)	M_Z (GeV)	Dominant fermion-loop approximation		Complete one-loop results Ref. 14, $m_H = 100$ GeV		Difference	
		M_W (GeV)	s_W^2	M_W (GeV)	s_W^2	ΔM_W (MeV)	Δs_W^2
30	88	75.69	0.2602				
	90	78.29	0.2433	78.29	0.2434	0	-0.0001
	92	80.81	0.2284	80.80	0.2287	10	-0.0003
	94	83.27	0.2152	83.26	0.2155	10	-0.0003
	96	85.69	0.2033	85.66	0.2038	30	-0.0005
60	88	75.72	0.2596				
	90	78.32	0.2428	78.27	0.2436	50	-0.0008
	92	80.84	0.2279	80.78	0.2291	60	-0.0012
	94	83.30	0.2147	83.22	0.2162	80	-0.0015
	96	85.71	0.2029	85.62	0.2046	90	-0.0017
90	88	75.90	0.2561				
	90	78.49	0.2394	78.47	0.2398	20	-0.0004
	92	81.01	0.2247	80.98	0.2253	30	-0.0006
	94	83.46	0.2116	83.43	0.2123	30	-0.0007
	96	85.87	0.1999	85.82	0.2008	50	-0.0009
130	88	76.12	0.2518				
	90	78.71	0.2351	78.70	0.2353	10	-0.0002
	92	81.23	0.2204	81.22	0.2207	10	-0.0003
	94	83.69	0.2073	83.67	0.2076	20	-0.0003
	96	86.11	0.1955	86.08	0.1959	30	-0.0004
180	88	76.47	0.2449				
	90	79.06	0.2283	79.06	0.2284	0	-0.0001
	92	81.59	0.2136	81.57	0.2138	20	-0.0002
	94	84.05	0.2005	84.04	0.2007	10	-0.0002
	96	86.47	0.1887	86.46	0.1889	10	-0.0002
230	88	76.91	0.2362				
	90	79.50	0.2197	79.52	0.2194	-20	0.0003
	92	82.03	0.2051	82.04	0.2047	-10	0.0004
	94	84.49	0.1920	84.52	0.1916	-30	0.0004
	96	86.92	0.1803	86.95	0.1797	-30	0.0006

Table 2

The radiative correction, $(\delta s_W^2)_{RC} = s_W^2 - s_B^2$, to be applied to s_B^2 , where s_B^2 is the weak angle extracted from neutrino scattering by using the Born approximation. The radiative correction is given for neutrino hadron (R_ν , R^+ , R^-) and neutrino electron scattering as a function of the top quark mass, m_t . We assume $M_Z = 91.8$ GeV, which together with α and G_μ fixes s_W^2 as shown in the Table. As for the momentum transfer, we assumed $\langle q^2 \rangle = 20$ GeV² for neutrino hadron and $\langle q^2 \rangle = 0.09$ GeV² for neutrino electron scattering. We note that the results for the case of neutrino electron scattering are unchanged if q^2 is varied between $q^2 = 0.01$ GeV² and $q^2 = 1$ GeV².

m_t (GeV)	s_W^2	R_ν (B = 5/9 × 1.39)		R^+	R^-	$\nu_\mu e / \bar{\nu}_\mu e$
		Present Calculation	Ref. 29	B = 10/9	B = 0	
		$(\delta s_W^2)_{RC}$	$(\delta s_W^2)_{RC}$	$(\delta s_W^2)_{RC}$	$(\delta s_W^2)_{RC}$	$(\delta s_W^2)_{RC}$
30	0.2298	-0.010	-0.010	-0.013	-0.007	-0.003
45	0.2295	-0.010	-0.009	-0.013	-0.007	-0.003
60	0.2293	-0.010	-0.008	-0.013	-0.007	-0.003
90	0.2261	-0.009	-0.010	-0.011	-0.007	-0.005
120	0.2229	-0.010	-0.011	-0.011	-0.008	-0.008
180	0.2150	-0.010	-0.011	-0.009	-0.011	-0.013
240	0.2045	-0.010	-0.011	-0.007	-0.014	-0.021

References

1. M. Veltman, Phys. Lett. 91B (1980) 95; M. Green, M. Veltman, Nucl. Phys. B 169 (1980)137; Erratum B175 (1980) 547.
2. F. Antonelli, M. Consoli, G. Corbò, Phys. Lett. 91B (1980) 90; F. Antonelli, G. Corbò, M. Consoli, O. Pelegriano, Nucl. Phys. B183 (1981) 475.
3. A. Sirlin, Phys. Rev. D22 (1980) 971; W. Marciano and A. Sirlin, Phys. Rev. D22 (1980) 2695.
4. S.L. Glashow, Nucl. Phys. 22 (1961) 579; S. Weinberg, Phys. Rev. Lett. 19 (1967) 1264; A. Salam, in Elementary Particle Theory, ed. N. Svartholm , Almquist and Wiksell, Stockholm 1968, p. 367.
5. W. Marciano, Phys. Rev. D20 (1979) 274.
6. F. Antonelli and L. Maiani, Nucl. Phys. B186 (1981) 269; S. Belucci, M. Lusignoli and L. Maiani, Nucl. Phys. B189 (1981) 329.
7. S. Dawson, J.S. Hagelin and L. Hall, Phys. Rev. D23 (1981) 2666.
8. For reviews see, e.g., L. Maiani, Topics in Intermediate Vector Boson Physics, Lectures given at Ann Arbor Summer School 1984 (unpublished); G. Altarelli, Acta Physica Austriaca, Suppl. XXIV (1982) 229; W. Hollik, in Progress in Electroweak Interactions, Vol. 1, ed. J. Tran Thanh Van (21st Rencontre de Moriond, 1986), Talk at the EPS Int. Conf. on High Energy Physics, Uppsala, Sweden (1987).
9. M. Veltman, Nucl. Phys. B123 (1977)89; M.S. Chanowitz, M.A. Furman and I. Hinchliffe, Phys. Lett. 78B (1978) 285.
10. J. Maalampi and M. Roos, Helsinki preprint HU-TFT 87-12; V. Barger et al., Madison preprint MAD/PH/3-41; I.I. Bigi and A.I. Sanda, SLAC-PUB-4269 (1987); J. Ellis, J.S. Hagelin and S. Rudaz, Minnesota preprint UMN-TH-602-87; H. Harari, SLAC-PUB-4327 (1987).
11. M. Chanowitz, M. Golden and H. Georgi, Phys. Rev. Lett. 57 (1986) 2344, Phys. Rev. D36 (1987) 1490.
12. B.W. Lee, C. Quigg and H.B. Thacker, Phys. Rev. D16 (1977) 1519; M. Chanowitz and M.K. Gaillard, Nucl. Phys. B261 (1985) 379.
13. M. Marciano and A. Sirlin, Phys. Rev. D29 (1984) 945.
14. B.W. Lynn and R.G. Stuart, Nucl. Phys. B253 (1985) 216.

15. F. Jegerlehner, Z. Phys. C32 (1986) 195, C32 (1986) 425.
16. U. Amaldi et al., Phys. Rev. D36 (1987) 1385.
17. P. Langacker, W. Marciano and A. Sirlin, Phys. Rev. D36 (1987) 2191.
18. P.Q. Hung and J.J. Sakurai, Nucl. Phys. B143 (1978) 81; J.D. Bjorken, Phys. Rev. D19 (1979) 335.
19. R. Kögerler and D. Schildknecht, CERN-TH 3231 (1982) (unpublished); M. Kuroda, D. Schildknecht and K.H. Schwarzer, Nucl. Phys. B261 (1985) 432; D. Schildknecht, in Electroweak Effects at High Energies, ed. H.B. Newman (Plenum Publishing Company 1985) p. 551; F. Schrempp and B. Schrempp, DESY 84-055 (1984) (unpublished).
20. F.M. Renard and D. Schildknecht, Phys. Lett. B183 (1987) 366.
21. M. Consoli, S. LoPresti and L. Maiani, Nucl. Phys. B223 (1983) 474.
22. W.J. Marciano and A. Sirlin, Phys. Rev. Lett. 46 (1981) 163; M.A.B. Beg and A. Sirlin, Phys. Rep. 88 (1982) 1.
23. S. Sarantakos and A. Sirlin, Nucl. Phys. B217 (1983) 84.
24. G. Costa, J. Ellis, G.L. Fogli, D.V. Nanopoulos and F. Zwirner, CERN-TH 4675/87.
25. D. Yu Bardin, S. Riemann and T. Riemann, Z. Phys. C32 (1986) 121.
26. L. di Lella, Proc. 1985 International Symposium on Lepton and Photon Interactions at High Energy, Kyoto (Japan 1985), ed. M. Konuma and R. Takahashi, Kyoto University; E. Locci, in Antiproton 86, ed. S. Charalambous et al., World Scientific; R. Amsari et al. (UA2), Phys. Lett. 186B (1987) 440; G. Arnison et al. (UA1), Phys. Lett. 166B (1986) 484.
27. Physics at LEP, CERN 86-02, Yellow Report, Vol. 1 and 2.
28. Polarized e^+ and e^- Beams at LEP, Working Group Report, CERN/LEPC/87-6 (1986).
29. J. Kiskis, Phys. Rev. D8 (1973) 2129; A. Sirlin and W.J. Marciano, Nucl. Phys. B189 (1981) 442; E.A. Paschos and M. Wirbel, Nucl. Phys. B194 (1982) 189; C.H.Llewellyn Smith and J.F. Wheeler, Phys. Lett. 105B (1981) 486, Nucl. Phys. B208 (1982) 27, B226 (1983) 547 (E).
30. C.H.Llewellyn Smith, Nucl. Phys. B228 (1983) 205.
31. D. Yu Bardin and V.A. Dokuchaeva, Dubna preprint E2-86-260 (1986)
32. R.G. Stuart, Z. Phys. C34 (1987) 445.

33. A. Sirlin, Rockefeller preprint RU 87/B1/10 (1987).
34. J. Bernstein and T.D. Lee, Phys. Rev. Lett. 11 (1963) 512; J.E. Kim, V.S. Mathur and S. Okubo, Phys. Rev. D9 (1974) 3050.
35. E.A. Paschos and L. Wolfenstein, Phys. Rev. D7 (1973) 91.
36. H. Abramowicz et al. (CDHS collaboration), Phys. Rev. Lett. 57 (1986) 298.
37. J.V. Allaby et al. (CHARM collaboration), Phys. Lett. 177B (1986) 446.
38. R.P. Feynman, Theory of Fundamental Processes, W.A. Benjamin, New York, 1962, p. VII.
39. G. 't Hooft, Nucl. Phys. B33 (1971) 173.
40. E.H. de Groot and D. Schildknecht, Z. Phys. C10 (1981) 55.

Figure Captions

Figure 1 : Fermion-loop diagrams contributing to the W and γZ propagators.

Figure 2 : The radiative correction factor Δr as a function of the top quark mass, m_t , in the dominant fermion-loop approximation of the present paper (full line) compared with a complete one-loop calculation²⁵⁾ for several values of the Higgs mass (broken lines). For the Z boson mass $M_Z = 93$ GeV has been used as input. (The shape of the curve for the dominant fermion-loop approximation for values of $m_t \approx M_W$ is an artefact of extrapolating the results for Δr obtained for $m_t \ll M_W$ and $m_t \gg M_W$ to the region of $m_t \approx M_W$. A more careful treatment can be carried out to improve the behaviour of Δr in the vicinity of $m_t \approx M_W$.)

Figure 3 : Diagrams describing neutrino scattering in the leading log approximation, (a) ordinary neutral current contribution, (b) neutrino charge radius contribution, (c) QED correction to charged current neutrino interactions.

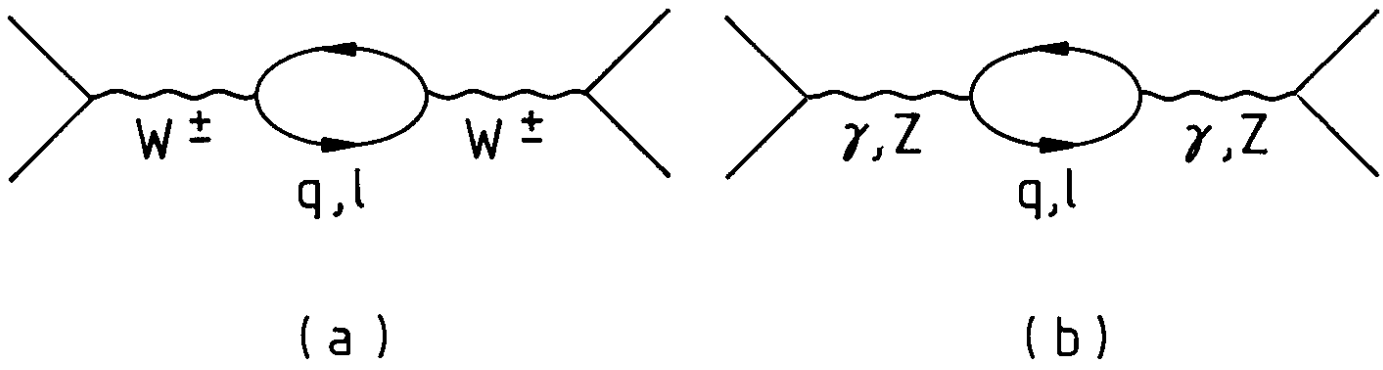


Figure 1

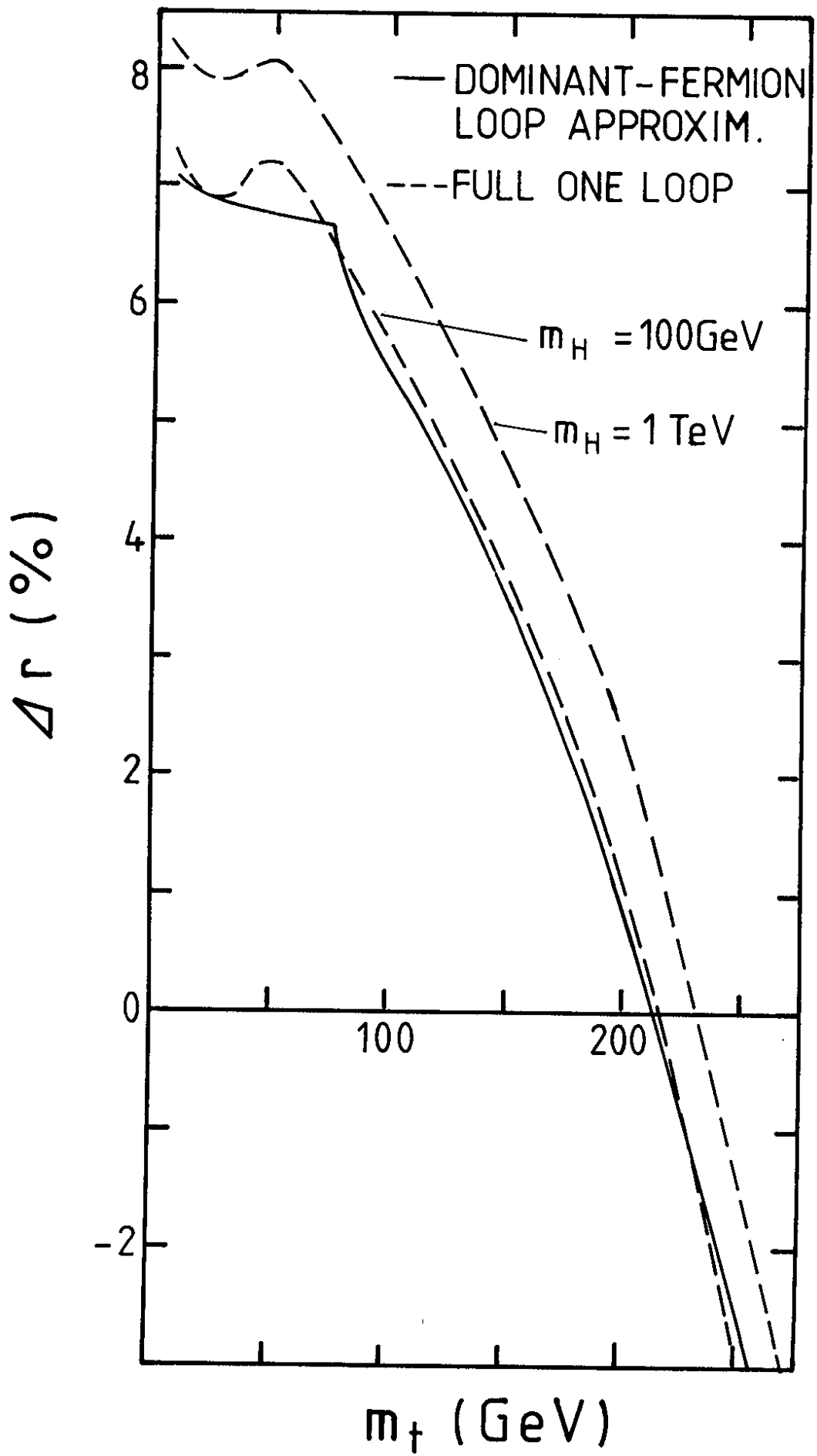
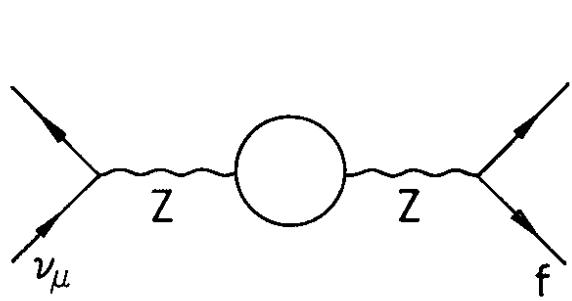
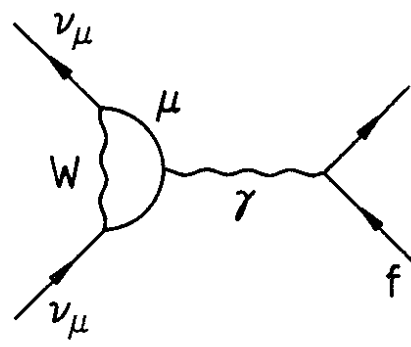


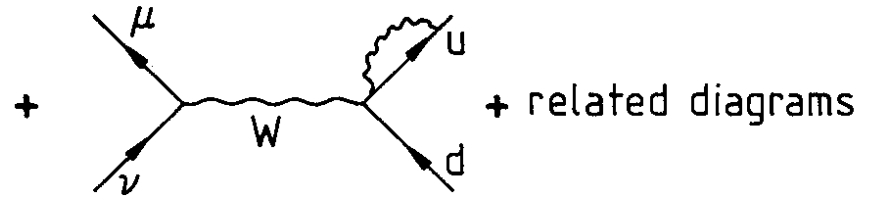
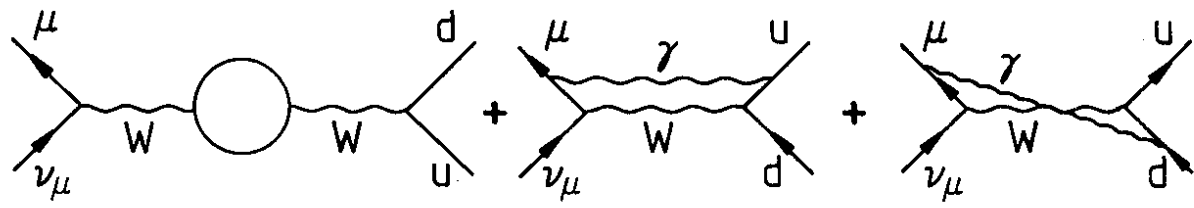
Figure 2



(a)



(b)



+ related diagrams

(c)

Figure 3